# SOIL MOISTURE CHANGE DUE TO VARIABLE WATER TABLE

A Thesis
Presented to
The Academic Faculty

by

Madhusudan S. Kamat

In Partial Fulfillment
of the Requirements for the Degree
Master of Science in the
School of Civil and Environmental Engineering

Georgia Institute of Technology
[DEC 2015]

# SOIL MOISTURE CHANGE DUE TO VARIABLE WATER TABLE

Approved by:

Dr. Jian Luo, Advisor
School of Civil and Environmental Engineering
*Georgia Institute of Technology*

Dr. Jingfeng Wang
School of Civil and Environmental Engineering
*Georgia Institute of Technology*

Dr. Aris P. Georgakakos
School of Civil and Environmental Engineering
*Georgia Institute of Technology*

Date Approved: [2 DEC 2015]

# ACKNOWLEDGEMENTS

I wish to thank Dr. Jian Luo for his continued support throughout my research. I would also like to thank my parents and my friends at Georgia tech for all the help they have rendered over the course of my time here. I would like to thank Abhinaya Shetty for help for all computer and software problems that I faced over the course of my researchI would like to take this opportunity to also thank the Office of Information Technology at Georgia Tech for their help on every problem that I faced.

# TABLE OF CONTENTS

# LIST OF TABLES

# LIST OF FIGURES

# SUMMARY

Soil moisture distribution varies with a fluctuating water table. This research was conducted to numerically model and investigate the dynamic process of soil moisture change with a periodically moving water table. A numerical model was developed with the use of COMSOL to simulate groundwater flow through an unsaturated-saturated medium. The medium was considered as homogeneous and isotropic. The model was generated by using the Richards' equation model from the subsurface flow module of COMSOL 4.4. The model uses the van Genuchten retention model.

The flow was assumed to be through uniform soil with homogeneous properties of hydraulics in all directions. The soil is variably saturated above the water table. The water table is varied with respect to time and space across the specimen. The change with time can be attributed to seasonal or diurnal variation.

The model results show the variation of moisture with depth of soil as time proceeds. The temporal variation is characterized by a rapid change in moisture in the soil depth near the water table, in comparison to the soil away from the water table. The moisture profiles for sand and gravel are compared for qualitative and quantitative differences.

# CHAPTER 1

# INTRODUCTION

The unsaturated zone is an integral part of the hydrological cycle, playing an important role in various aspects such as groundwater runoff, infiltration and soil moisture storage. Hence, the vadose zone is studied, to understand the effect of fertilizers and pesticides and their movement below the soil root zone on the underlying groundwater reservoirs. A variety of analytical and numerical models are used to study the water and solute transport between the water table and ground surface. The most popular among them is the Richards' equation, which studies flow of fluid through variably saturated soil. It has been used to predict water and solute movement in the unsaturated vadose zone and for obtaining information through extrapolation of observations from a limited number of field experiments.

Over the course of time, the water table rises and drops due to the seasonal changes in water inflow to the groundwater table, increase or decrease in evaporation and a variation in the runoff. This report uses the Richards' equation feature in the sub-surface module of COMSOL 4.4 to model the variation of moisture content in the soil due to the periodic variation of water table over varying periods. The modelling is done with some basic assumptions in mind:

(i) The soil is homogeneous and isotropic.

(ii) The rainfall or infiltration rate is constant.

In the field however, the soils are never completely homogeneous. Usually soils may contain smaller rocks or some amount of other types of soil. It is also very rare for the

initial moisture content of the soil sample to be uniform. But prediction of moisture movement under field boundary conditions is complicated and needs models which can handle non-homogeneity of the soil. Such predictions are essential in the study of transport of fertilizers, pesticides and for vapor intrusion.

The current study however, only undertakes the temporal variation of soil moisture with respect to the change in water table levels on a diurnal, weekly and yearly basis. Various cases have been undertaken so as to diminish the effects of non-homogeneity as well as the variation in initial moisture content.

# CHAPTER 2

# LITERATURE REVIEW

Groundwater movement can take place due to a large variety of reasons involving agricultural, environmental, industrial and hydrological processes. These may include, but are not restricted to, irrigation, runoff, rainfall, evapotranspiration and drawdown. Hence, it is crucial to know how to predict groundwater level, so as to exploit it to the best of our ability. It is essential that water is withdrawn sustainably, so as to avoid any undesirable effects such as reservoir exhaustion, excessive pumping or water quality decline.

Water table rise occurs as a result of recharge to the reservoir in groundwater basins. The problem of groundwater flow modelling and its prediction, is the vertical recharge it receives from the underlying aquifer and the parallel streams and drains. The head and discharge variation with respect to time is impacted by the unsteady flow of groundwater. Various researchers have tried to implement different solutions for the same. Hammad [1969] was one of the foremost to discuss the problem through his research about the groundwater resources in African Sahara. He addressed the problem by a system of wells placed collinearly and then replaced that system by a 2-D ditch. Werner [1959] studied groundwater flow in an unconfined aquifer receiving recharge and developed expressions that include the effect of different levels of water levels in the drains. Massland [1959] presented a detailed analysis of the effect on the water table of intermittent recharge. In both these cases, the results are presented in the form of an infinite series.

Gill [1981] improved on Hammad's research to modify the initial and boundary conditions. He framed a solution for transient flow under from a ditch to an aquifer under unsteady conditions. He found that after a theoretical infinite time passage, a steady state is achieved. Mustafa [1983] introduced the terms of infiltration and evaporation in a semi-confined aquifer by considering a recharge source and ditch on the sides of the aquifer. He found the unsteady state solution for the system by the use of a Fourier series and compared the same with the results of Gill by using the Laplace method. He found that his Fourier series was suited for larger time values while the solution of Gill was better suited for smaller time values. Ram et al [1994] verified these results by using a different analytical solution and vertical infiltration.

Venetis [1971] arrived at a plausible estimation of infiltration by considering it as a constant with respect to distance, but a step function with respect to time. Onyejekwe determined the response of a system with an unsteady flow of water from a leaky aquifer with an external source. He found the solution of a 1-D horizontal flow and found that the no-flow boundary condition does not have as much influence below a certain threshold.

Mustafa [1987] introduced the trapezoidal, parabolic, exponential and periodic recharge functions. The aquifer considered was bounded by two ditches of equal levels at the initial position. Then, the level of water was lowered and maintained at the same level and the system was analyzed with the use of each of the four recharge functions mentioned earlier. He observed that the results were comparable for plots of head against distance.

Latinopoulos [1981] gave an analytical solution for the problem for the seasonal variation of groundwater flow in an unconfined aquifer under artificial recharge. An

optimum solution can be given by an efficient distribution of the recharge rate in both storage and outflow.

Over the course of a year, the water table fluctuation remains more or less constant. This is due to the evapotranspiration, plant uptake and runoff being compensated by the precipitation occurring in the area. Variation in depth of water table is usually not high in soils with one kind of soil as seen by Lyford [1964]. Usually the yearly variation of water table level depends on the amount and temporal spacing of precipitation over the area.

The following summarizes the modelling method and model details used for this research.

## MODELLING FOR RICHARDS EQUATION IN VARIABLY SATURATED CONDITION:

Variably saturated flow is governed by equations such as the Richards' equation and the Darcy-Buckingham equation. The Richards' equation combines the Darcy-Buckingham equation for fluid flux with a mass balance equation.

Water flow in variably saturated soils can be represented by a mass balance or the continuity equation as follows:

$$\frac{\partial \theta}{\partial t} = -\frac{\partial q}{\partial z}$$

…….Eqn 2.1

Where Θ is the water content per unit volume [$L^3L^{-3}$]

T is the time [T]

$q_i$ is the flux density per volume [$LT^{-1}$]

The mass balance equation shows that a spatial change in water flux or a sink/source causes a change in water content in the soil. This is due to the water flux in and out of the given soil volume.

The uniform flow in soils can be described by the Darcy-Buckingham equation:

$$q_i = -K(h)(K_{ij}^A \frac{\partial h}{\partial x_j} + K_{iz}^A)$$

…….Eqn 2.2

Where K is the unsaturated hydraulic conductivity [$LT^{-1}$]

$K^{Aij}$ are components of a dimensionless anisotropy tensor $K^A$

Combining the mass balance equation and the Darcy-Buckingham equation gives the general Richards equation:

$$\frac{\partial \theta}{\partial t} = \frac{\partial}{\partial xi}\left[K\left(K_{ij}^A \frac{\partial h}{\partial x_j} + K_{iz}^A\right)\right] - S$$

…….Eqn 2.3

Where,
$X_i$ is the spatial coordinate [L]

$\Theta$ is the water content [$L^3L^{-3}$]

S is the sink term [$L^3L^{-3}T^{-1}$]

t is time [T]

h is the pressure head [L]

$K_{ij}^A$ and $K_{iz}^A$ are components of a dimensionless anisotropy tensor $K^A$

K is the unsaturated hydraulic conductivity [$LT^{-1}$]

K is given by $K(h,x,z) = K_s(x,z)K_r(h,x,z)$

Where $K_r$ is the relative hydraulic conductivity and $K_s$ is the saturated hydraulic conductivity [$LT^{-1}$].

The anisotropy tensor $K_{ij}^A$ is used to account for an anisotropic medium. It can be defined by a unit tensor for an isotropic medium.

This report documents the use of the Richards' equation module of COMSOL 4.4 for simulating water movement in a two-dimensional variably saturated media. Comsol numerically solves the Richards' equation for unsaturated water flow.

For the problem that has been considered, the groundwater is open to the surface and hence the water is under atmospheric pressure. In such a case, the governing equation is the Richards equation for pressure head as given by J Bear:

$$[C + S_e S]\frac{\partial H_p}{\partial t} + \nabla.\left[-K\nabla\left(H_p + D\right)\right] = 0$$

…….Eqn 2.4

where C denotes specific moisture capacity ($m^{-1}$);

Se is the effective saturation of the soil (dimensionless);

S is a storage coefficient ($m^{-1}$);

Hp is the pressure head (m), which is proportional to the dependent variable, p (Pa);

t is time;

K equals the hydraulic conductivity (m/s);

D is the direction (typically, the z direction) that represents vertical elevation (m).

Comsol converts the Richards equation to SI units so as to solve for the pressure (in Pa). The hydraulic head, pressure head and elevation are dependent on the pressure p as follows:

$$H = H_p + D$$

$$H_p = \frac{p}{\rho g}$$

The permeability κ ($1/m^2$) and the hydraulic conductivity K (m/s) can be related to the viscosity μ (Pa.s) and density ρ ($kg/m^3$) of the fluid and the acceleration due to gravity g ($m/s^2$) by

$$\frac{\kappa}{\mu} = \frac{K}{\rho g}$$

…….Eqn 2.5

The volumetric fraction of water is given by the van Genuchten formula as:

$$\Theta = \begin{cases} \Theta_r + S_e(\Theta_s - \Theta_r) & H_p < 0 \\ \Theta_s & H_p \geq 0 \end{cases}$$

…….Eqn 2.6

When the fluid pressure is equal to the atmospheric pressure, the soil is considered to be saturated ($H_p=0$).

C, $S_e$ and K varies with $H_p$ and Θ. The specific moisture capacity C relates moisure in soil to the pressure head $H_p$ as:

$$C = \frac{\partial \Theta}{\partial Hp}$$

C defines storage changes by varying fluid content as

$$C \frac{\partial Hp}{\partial t} = \frac{\partial \Theta}{\partial t}$$

…….Eqn 2.7

Thus, the storage coefficient C addresses storage changes due to compression and expansion of the pore spaces and the water when the soil is fully wet.

In this problem,

$$S= (\Theta_s – \Theta_r)/ (1[m]. \rho.g)$$

where $\Theta_s$ and $\Theta_r$ denote the volume fraction of fluid at saturation and after drainage, respectively.

Comsol uses the following van Genuchten formulae to represent how the four retention and permeability properties—Θ, *C*, Se, and $k_r=K/K_s$—vary with the solution $H_p$.

$$\Theta = \begin{cases} \Theta_r + S_e(\Theta_s-\Theta_r) & H_p< 0 \\ \Theta_s & H_p \geq 0 \end{cases}$$

$$S_e = \begin{cases} \frac{1}{[1+|\alpha H_p|^n]^m} & H_p< 0 \\ 1 & H_p \geq 0 \end{cases}$$

$$C= \begin{cases} \frac{\alpha m}{1-m}(\theta s - \theta r)S_e^{\frac{1}{m}}\left(1 - S_e^{\frac{1}{m}}\right)^m & H_p<0 \\ 0 & H_p\geq 0 \end{cases}$$

$$K_r= \begin{cases} S_e^{l}[1-(1-S_e^{1/m\ m})^{2}] & H_p<0 \\ 1 & H_p\geq 0 \end{cases}$$

In a two-dimensional, isothermal, variably saturated, rigid, porous medium with Darcian flow of water the liquid flow process if governed by the Richards equation given by:

$$\frac{\partial \theta}{\partial t} = \frac{\partial}{\partial xi}\left[K\left(K_{ij}^{A}\frac{\partial h}{\partial x_j} + K_{iz}^{A}\right)\right] - S$$

…….Eqn 2.8

Where,

Θ is the water content $[L^3L^{-3}]$

S is a sink term [$T^{-1}$]

t is time [T]

h is the pressure head [L]

$K_{ij}^A$ and $K_{iz}^A$ are components of a dimensionless anisotropy tensor $K^A$

K is the unsaturated hydraulic conductivity [$LT^{-1}$]

K is given by $K(h,x,z) = K_s(x,z)K_r(h,x,z)$

Where $K_r$ is the relative hydraulic conductivity and $K_s$ is the saturated hydraulic conductivity [$LT^{-1}$].

The anisotropy tensor $K_{ij}^A$ is used to account for an anisotropic medium. It can be defined by a unit tensor for an isotropic medium.

**Sink Term:**

The sink term S represents the volume of water removed per time from a unit volume of soil due to plant water uptake.

$$S(h) = a(h)S_p$$

where $S_p$ is the plant water uptake rate.

The water stress response function a(h) is a dimensionless function of the soil pressure head ($0 \leq a \leq 1$) (Feddes et al 1978)

Fig 3.1 gives the variation of the stress response function used by Feddes [1978]. As seen, the uptake rate is zero at saturation is at anaerobiosis point $h_1$. The uptake is zero also when the plant is at wilting stage ie it has wilted at stage $h_4$. The uptake for the plant is optimal between $h_2$ and $h_3$ and it goes on decreasing beyond both those points linearly. Thus, the water uptake rate is equal to $S_p$ when a(h)=1.

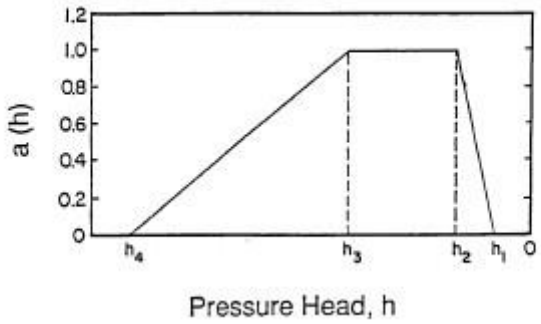


Figure 2.1: Schematic of plant water stress function, a(h) as used by Feddes et al [1978].

Over a 2-dimensional rectangular area, $S_p$ is given by

$$S_p = \frac{1}{L_x L_z} L_t T_p$$

Where $T_p$ is the potential transpiration rate [$LT^{-1}$]

$L_t$ is the root zone depth

In this study relationships proposed by van Genuchten are used (1980) to describe the unsaturated soil hydraulic properties.

**Van Genuchten Parameters:**

The parameter α represents the thickness of the capillary fringe and the parameter n represents the pore size distribution for the soil. α and n play an important role in the moisture movement through the vadose zone.

As the value of α increases the capillary fringe thickness reduces. A lower α value soil retains greater amount of water in the unsaturated zone due to its capillary forces.

The width of pore size distribution increases with a decrease in the value of parameter n. Thus, as the value of n reduces, the relative abundance of small pores increases. This makes the soils difficult to drain as a result of their viscous forces. The hydraulic

conductivity decreases as the n increases till a point. Beyond the point, the hydraulic conductivity increases with n.

**Calculation of van Genuchten Parameters:**

The van Genuchten retention model is given by the equation:

$$\frac{\theta - \theta_r}{\theta_s - \theta_r} = [1 + (\alpha|h|)^n]^{-m}$$

…….Eqn 2.9

Shao and Horton (1998) described the soil water potential profile during infiltration by a Mclaurin's function:

$$H=\alpha_0 + \alpha_1\lambda + \alpha_2\lambda^2 + \ldots.$$

where $\lambda$ is the Boltzmann transformation variable with $\lambda = x/t1/2$, where $x$ is the horizontal distance and $t$ is the infiltration time. The Boltzmann variable helps to transform the eqn 2.9 which is a PDE into an ODE. Shao and Horton (1998) solved the Richards' equation by an integral method.

$$\frac{\partial\theta}{\partial t} = \frac{\partial}{\partial x}\left[k(\theta)\frac{\partial h}{\partial x}\right]$$

…….Eqn 2.9

Where k(Θ) is the unsaturated water conductivity as a function of moisture content. The solution of this equation can be used to calculate the van Genuchten parameters. Shao and Horton (1998) solved for n and α by combining the equation with Darcy's flow equation.

$$n = \frac{S}{d(\theta s - \theta i) - S}$$

$$\alpha = \frac{2k_s}{Sd}\left[\frac{1}{m}\left(\frac{\theta s - \theta i}{\theta s - \theta r}\right)\right.$$

…….Eqn 2.10

Where $\Theta_i$ is the initial water content ($cm^3\ cm^{-3}$), $k_s$ is the saturated water conductivity (cm/min), *d* is the characteristic wetting length of the horizontal soil column which is the wetting front distance divided by $t^{1/2}$ ($cm/min^{1/2}$), and *S* is the sorptivity, which is the slope of the infiltration rate *q* (cm/min) *versus* $1/(2t^{1/2})$, that is,

$$q = \frac{S}{2t^{1/2}}$$

**Numerical Scheme for Richards' Equation:**

The Richards' equation can be solved by using a Galerkin finite element discretization in time.

To achieve the same, the domain is discretized into M-1 elements of length Δz with M nodes. The pressure head h is calculated as:

$$h(z,t) = \Sigma h_m(t) N_m(z)$$

where $h_m(t)$ are unknown global nodal values of h and $N_m(z)$ are the corresponding Lagrangian basis functions.

Using Galerkin formulation on Richards' equation gives:

$$A(h)h+F(h)dh/dt +b(h)-q(t)=0$$

…….Eqn 2.11

Where h is the vector of unknown coefficients of the pressure head at each node

q is the flux boundary condition at lower and upper boundary

A, F and b over a local element $x^{\epsilon}$ are given by the equations:

$$A^{(e)} = \int_{xe}^{0} K^{e} \frac{\partial N1e}{\partial z} \frac{\partial Nme}{\partial z} dz$$

$$F^{(e)} = \int_{xe}^{0} C^{(e)} N_1^{(e)} N_m^{(e)} dz$$

$$B^{(e)}=\int_{xe}^{0} K^{(e)} \frac{\partial N1e}{\partial z} dz$$

…….Eqn 2.12

For $-1 \leq \varepsilon \leq 1$,

$N^{(e)1}= 0.5(1-\varepsilon)$

$N^{(e)m}=0.5(1+\varepsilon)$,

Where $\varepsilon = 2(z-z^{(e)}_c)/\Delta z^{(e)}$

And z is the coordinate of a point in the sub-domain element w

$z^{(e)c}$ and $z^{(e)}$ are the coordinates of the midpoint and length of element $x^{(e)}$.

**Time differentiation:**

With a backward finite difference discretization of the time derivative term Eqn 2.11 can be written as:

$A(h^{k+\lambda t}) h^{k+\lambda t} + F(h^{k+\lambda t})(h^{k+1}-h^{k})/\Delta t + b(h^{k+\lambda t})-q(h^{k+\lambda t}) = 0$ …….Eqn 2.13

Where

$h^{k+\lambda t} = \lambda_t h^{k+1} + (1-\lambda_t) h^{k}$ ….. $0 \leq \lambda_t \leq 1$

In eqn 2.13 k denotes the time level, $\Delta t$ denotes the time step and $\lambda_t$ denotes the time weighting or relaxation parameter. Eqn are nonlinear $h^{k+1}$ except when $\lambda_t = 0$.

**Picard Scheme:**

The Picard scheme on eqn 2.13 by iterating at previous level p:

$[\lambda_t A^{k+\lambda t,p} + 1/\Delta t.\ F^{k+\lambda t,p}]\ h^{k+1,p+1} = q^{k+\lambda t,p} – b^{k+\lambda t,p} – (1-\lambda_t)\ A^{k+\lambda t,p} h^{k} + 1/\Delta t\ F^{k+\lambda t,p}\ h^{k}$

This equation can be written as:

$[\lambda_t A^{k+\lambda t,p} + 1/\Delta t.\ F^{k+\lambda t,p}]\ \Delta h^{k+1,p+1} = -f(h^{k+1,p})$ …….Eqn 2.14

Where

$\Delta h^{k+1,p+1} = h^{k+1,p+1} - h^{k+1,p}$

And $f(h^{k+1,p}) = \lambda_t A^{k+\lambda t,p} h^{k+1,p} + (1-\lambda_t)A^{k+\lambda t,p} + F^{k+\lambda t,p} [(h^{k+1,p} - h^k)/\Delta t] + b^{k+\lambda t,p} - q^{k+\lambda t,p}$

Equation 2.14 is valid for the Neumann boundary condition with a specified flux, but has to be modified for the Dirichlet boundary condition.

**Lenhards' Equation:**

Lenhard et al (1989) related the Brookes and Corey and van Genuchten models by equating the differential fluid saturation capacities, dSe/dh, of the two models to obtain the following relationship between the BC model pore size distribution index λ and the vG model parameter m:

$$\lambda = \frac{m}{1-m}\left(1 - S_e^{\frac{1}{m}}\right)$$

…….Eqn 2.15

Evaluating dSe/dh at the midway, when Se = 0.5,

$$\lambda = \frac{m}{1-m}\left(1 - 0.5^{\frac{1}{m}}\right)$$

…….Eqn 2.16

From the Brooks-Corey and Tyler and Wheatcraft (1990) model,

$$\lambda = 3 - D$$

Where D is the fractal dimension

Hence,

$$D = 3 - \frac{m}{1-m}\left(1 - 0.5^{\frac{1}{m}}\right)$$

…….Eqn 2.17

Assuming large values of h, we get,

$\lambda = n-1$

and m=1-1/n

Hence, m=(3-D)/(4-D)

Lenhard suggested the following relationship between $h_{min}$ and the can Genuchten parameter α:

$$\alpha = \frac{S_x^{\frac{1}{\lambda}}}{h_{min}}(S_x^{-\frac{1}{m}} - 1)^{1-m}$$

…….Eqn 2.18

where $S_x$ is the effective wetting phase saturation at match-point given by:

$$S_x = 0.72 - 0.35\exp(-n^4)$$

…….Eqn 2.19

# CHAPTER 3

# METHOD

## OBJECTIVE OF RESEARCH:

As stated earlier, the objectives of this dissertation are to:

1] Study the variation of soil moisture content due to the change in groundwater table.

2] Develop a model to study the temporal changes in soil moisture content.

## APPROACH:

The research involved the development of a model to calculate the saturation of soil at various points in a soil sample. The soil sample was fixed to be of a size of 5m wide and 4m deep. The water table was varied temporally and the subsequent saturation level was calculated at different depths of the soil sample. Richards' equation was used to calculate the water content at any given point in the soil sample. The model was tested on soils of different hydraulic conductivity ($K_s$), porosity ($\Theta$) and van Genuchten parameters ($\alpha$ and n). The effect of the water table variation was plotted for each case so as to understand the sensitivity of the model towards each parameter.

**SAMPLE:**

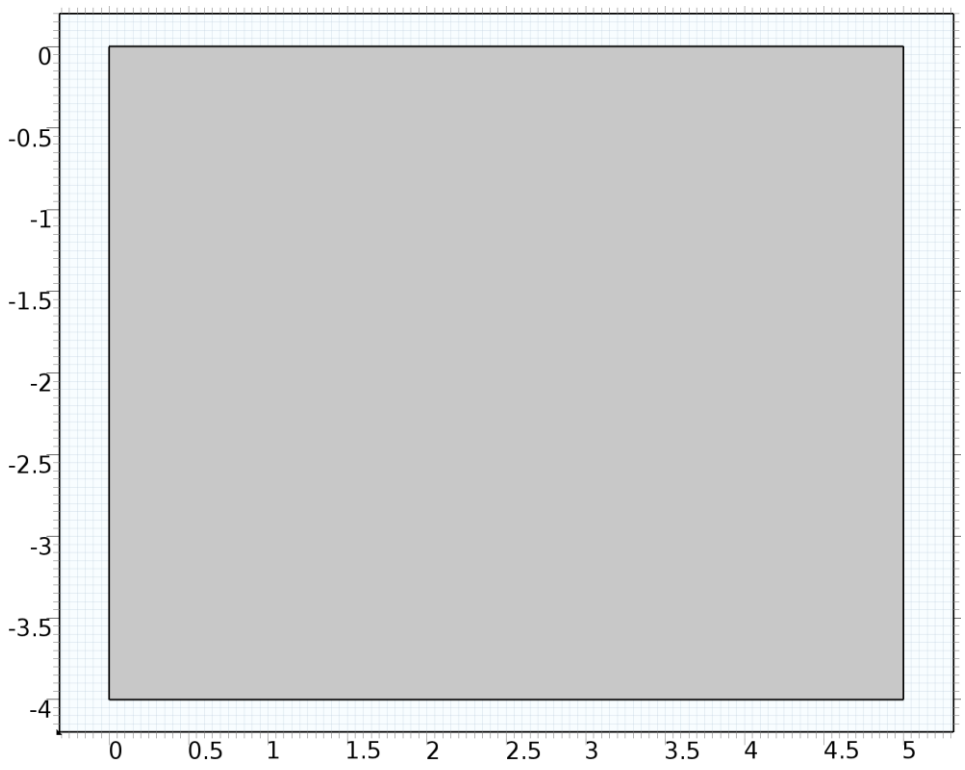


Fig 3.1: Size of soil sample for testing

The sample is a block of soil of width 5m and depth 4m. It is assumed to be homogeneous and isotropic with all its properties remaining constant in all directions during the entire test.

There is no mass flux along the sides, with the top being open. The only mass flux allowed is through the bottom of the sample with a flux of:

$N_0 = -K_s . \rho$

…….eqn 3.1

where,

$N_0$ is the inward mass flux;

$K_s$ is the hydraulic conductivity;

And $\rho$ is the density of fluid.

The pressure varies under the surface with a variation in depth. The initial pressure head was thus assumed to be:

Pressure Head = 0.5 m.

Thus, the water level was at 0.5 m in the initial or starting position. As we are plotting the variation of soil moisture temporally, the pressure head is varied with respect to time.

For the plot of yearly variation in the soil moisture the pressure varies temporally with a pressure head variation of:

$H_{p0}$ = 0.5-0.5*cos(2*pi/365*t [d])

…….eqn 3.2

The pressure head for the weekly variation plot varies as:

$H_{p0}$ = 0.5 – 0.5*cos(2*pi/7*t [d])

…….eqn 3.3

The pressure head for daily variation plot varies as:

$H_{p0}$ = 0.5 – 0.5*cos(2*pi/24*t [h])

…….eqn 3.4

To check for different initial pressure head conditions, the value for pressure head was varied as 0.5 m, 1 m and 2 m.

As the pressure varies, the water table rises or falls according to the rise or fall in pressure throughout the year. This results in a change in saturation throughout the sample. The saturation in the soil ie the moisture content is calculated by the use of Richards' equation.

Comsol 4.4 provides a module for the Richards' equation in its subsurface flow module.

**Boundary conditions:**

Thus, the boundary conditions for the sample are as follows:

Surface: n.u = 0

Sides: n.u = 0

Base: n.ρ u = $N_0$

**Richards' Equation on the Sample:**

$$[C + S_e S]\frac{\partial H_p}{\partial t} + \nabla.\left[-K\nabla\left(H_p + D\right)\right] = 0$$

…….eqn 3.5

The Richards' equation used in Comsol calculates the pressure head $H_p$ which is used to calculate the moisture content or the soil saturation using van Genuchten equations.

The values of the van Genuchten parameters and other hydraulic properties such as hydraulic conductivity, porosity and density varies for different types of soil. Hence to calculate the saturation level for different types of soil due to the variation in water table levels, it is necessary to know the values of each of these parameters for different soils.

The hydraulic conductivity depends on the soil grain size, the structure of the soil matrix, the type of soil fluid, and the relative amount of soil fluid (saturation) present in the soil matrix. The important properties relevant to the solid matrix of the soil include pore size distribution, pore shape, tortuosity, specific surface, and porosity. In relation to the soil fluid, the important properties include fluid density, and fluid viscosity. For a subsurface

system saturated with the soil fluid, the hydraulic conductivity, *K*, can be expressed as follows (Bear 1972):

$$K = \frac{k\rho g}{\mu}$$

Where *k*, the intrinsic permeability of the soil, depends only on properties of the solid matrix, and *g*, called the fluidity of the liquid, represents the properties of the percolating fluid. The hydraulic conductivity, *K*, is expressed in terms of length per unit of time ($LT^{-1}$), the intrinsic permeability, *k*, is expressed in $L^2$, and the fluidity, *g*, in $L^{-1}T^{-1}$.

For the current study, the values of hydraulic conductivity were taken from Freeze and Cherry (1979) and from Domenico and Schwartz (1990). These values were:

Table 3.1: Hydraulic conductivity of soil for different soil types

| **Soil Type** | **$K_s$ (m/s)** |
|---|---|
| Gravel | $3 \times 10^{-4}$ to $3 \times 10^{-2}$ |
| Sand Coarse | $9 \times 10^{-7}$ to $6 \times 10^{-3}$ |
| Sand Medium | $9 \times 10^{-7}$ to $5 \times 10^{-4}$ |
| Sand Fine | $2 \times 10^{-7}$ to $2 \times 10^{-4}$ |
| Silt | $1 \times 10^{-9}$ to $2 \times 10^{-5}$ |
| Clay | $1 \times 10^{-11}$ to $4.7 \times 10^{-9}$ |

Soil porosity (n) is the ratio of the volume of voids to the total volume of the soil. The soil porosity depends on the consistence and packing of the soil. It is directly affected by compaction. USCS gives different values of porosity for different types and grades of soil.

The following table gives values of porosity given by Morris and Johnson (1967) and by the USCS:

Table 3.2: Porosity of soil for different values of porosity

| Type of Soil | Morris and Johnson | USCS |
|---|---|---|
| Gravel | 0.25 to 0.40 | 0.23 to 0.38 |
| Sand Coarse | 0.31 to 0.46 | 0.26 to 0.43 |
| Sand Medium | 0.29 to 0.49 | N/A |
| Sand Fine | 0.26 to 0.53 | 0.29 to 0.46 |
| Silt | 0.34 to 0.61 | 0.29 to 0.52 |
| Clay | 0.34 to 0.57 | 0.5 to 0.75 |

The van Genuchten method is the most commonly used method for water retention curves in unsaturated soil. The van Genuchten function is given by:

$$S_e = \frac{1}{[1+|\alpha Hp|^n]^m}$$

…….eqn 3.6

where

Se is the effective saturation and calculated by Se = (θ − θr)/(θs − θr),

where θ is the water content (cm3 cm−3),

θr is the residual water content,

and θs is the saturated water content,

and α (kPa−1), n and m (m = 1 − 1/n) are empirical parameters.

The two van Genuchten parameters play an important role in the moisture movement through the vadose zone. α is a measure of the thickness of the capillary fringe, while n is an indication of the pore size distribution of the soil.

USCS gives the standard values for each parameter by calculating the values for n by the Lenhard method (1989) and substituting the same to find the value of α by using Lenhards' equation. These values vary according to the type of soil and the soil conditions.

Table 3.3: van Genuchten parameters for different types of soil

| Type of Soil | α (1/m) | n |
|---|---|---|
| Gravel | 20 | 4.23 |
| Sand Coarse | 14.5 | 2.68 |
| Sand medium | 12.4 | |
| Sand fine | 7.5 | |
| Silt | 2 | 1.37 |
| Clay | 0.8 | 1.09 |

The storage coefficient is calculated using:

$$S = \frac{\theta s - \theta r}{1[m].\rho.g}$$

where $\Theta_s$ and $\Theta_r$ denote the porosity and the residual saturation after drainage respectively and ρ is the density of water.

For the study, the residual saturation is kept constant as 0.001.

Table 3.4: Values for all parameters used for research

| Parameter | Value | Description |
|---|---|---|
| $\rho$ | 1000 kg/$m^3$ | Bulk desity of water |
| $\Theta_s$ | Variable | porosity |
| $\Theta_r$ | 0.001 | Residual saturation |
| $S_s$ | $(\Theta_s - \Theta_r)/ (1[m]. \rho.g)$ | Storage coefficient |
| $K_s$ | variable | Saturated hydraulic conductivity |
| $\alpha$ | Variable | Van Genuchten parameter $\alpha$ |
| n | Variable | Van Genuchten parameter n |
| $N_0$ | 0.01 x $K_s$ x $\rho$ | Inside flux from the bottom |

For the study, the sample was divided into smaller elements in the form of a mesh. This mesh was chosen to be in the form of triangles with fine elements of size 0.25 m equilateral triangles.

The study was conducted for a time duration of 365 days by calculating the pressure head for each day and then calculating the respective saturation for the depth at the time.

# CHAPTER 4

# MODEL VALIDATION

The model was validated by comparing its results with the results obtained from the model used by Neuman [1974]. The problem considers infiltration of a homogeneous soil column which is initially dry.

The parameters of the soil are:

$\alpha = 4.1\ m^{-1}$

n=1.964

$K_s = 7.22 \times 10^{-5}$ m/s

$\Theta_s = 0.35$

$\Theta_r = 0.02$

The initial pressure head of the soil is taken as -1.5 m. The column is subjected to a Dirichlet boundary condition at the soil surface, which results in vertical water flow. The model uses a fine grid approximation with $\Delta z = 1$ cm.

The saturation was plotted against the y coordinate to give the following graph:

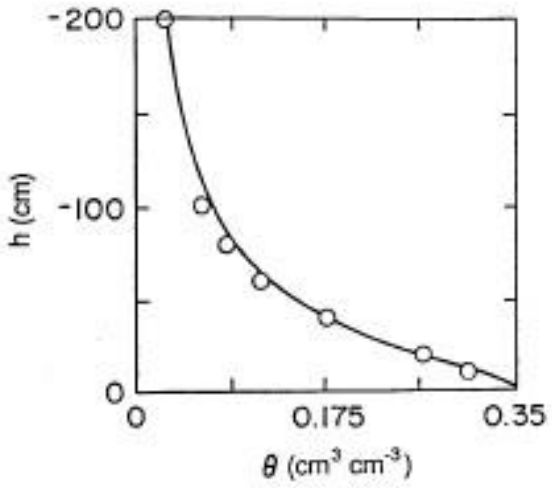


Fig 4.1: Depth vs saturation for Neuman's model

The same case has been plotted on the current model to give the following result:

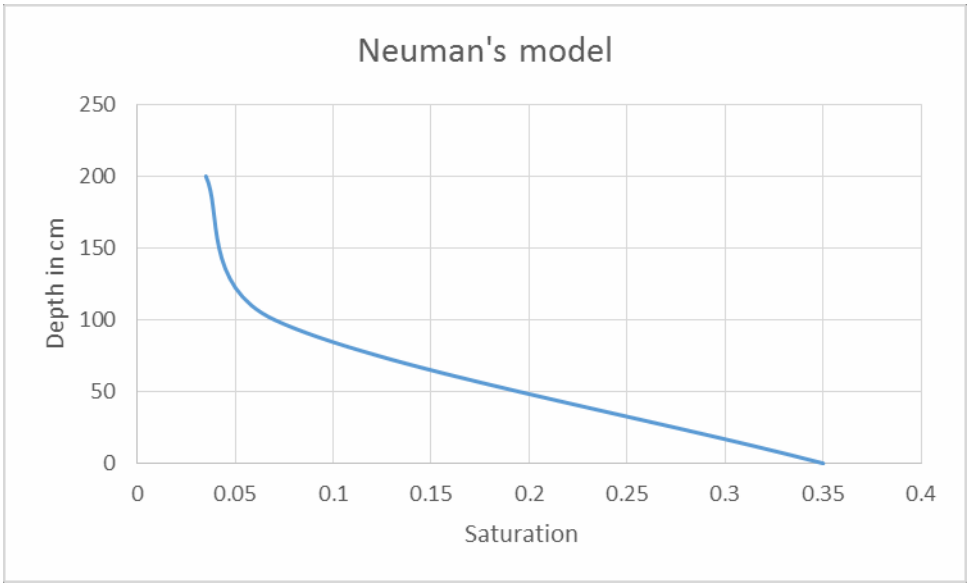


Fig 4.2: Neuman's model plotted on current model

The comparison of the two graphs shows that the error percentage is very low. This error may be attributed to the difficulty in presenting the simulation made by Neuman in the current model.

# CHAPTER 5

# RESULTS

## For Sand:

For plotting the temporal variation of moisture in the model of sand, the model was subjected to varying pressure head with all the other parameters constant at the following values:

$K_s = 9.22 \times 10^{-5}$ m/s

Porosity = 0.368

Residual saturation ($\Theta_r$) = 0.102

$\alpha = 3.35$

n = 2

The temporal variation was done on three levels: diurnal, weekly and yearly. While the soil profile shapes remain similar, there is a change in the top soil saturation levels for each case.

**DIURNAL VARIATION:**

**Case 1: Water table at 3.5 m depth:**

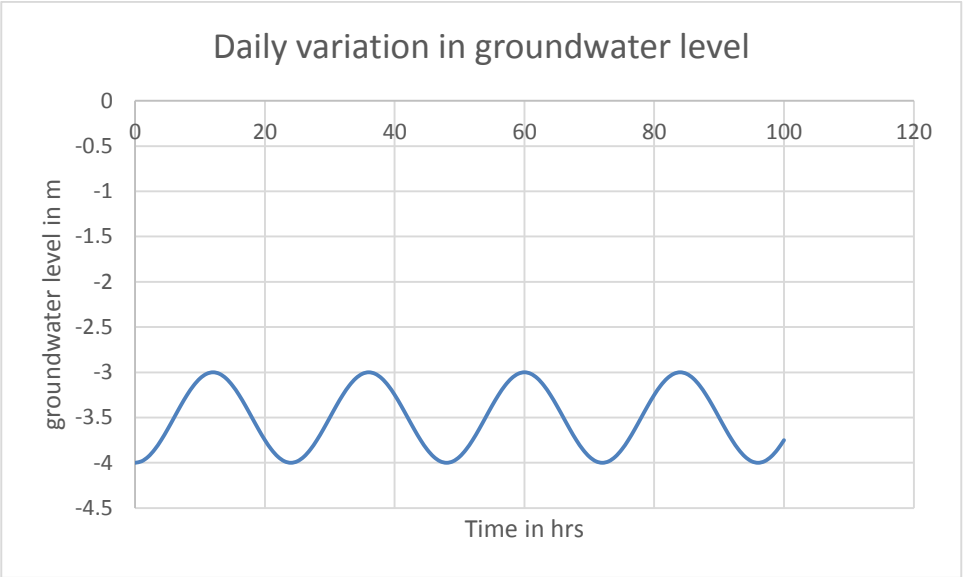


Fig 5.1: Daily variation in groundwater level at depth of 3.5 m

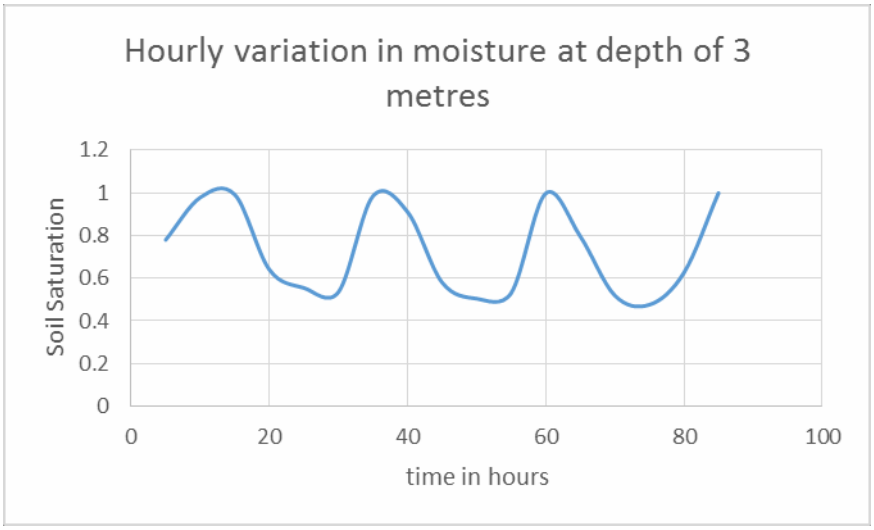


Fig 5.2: Hourly variation in moisture at depth 3 meters in sample for case 1

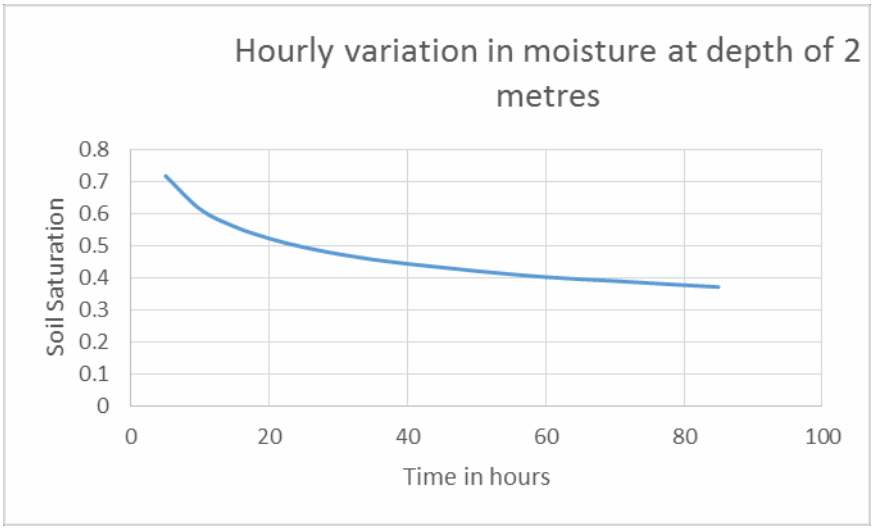


Fig 5.3: Hourly variation in moisture at depth 2 meters in sample for case 1

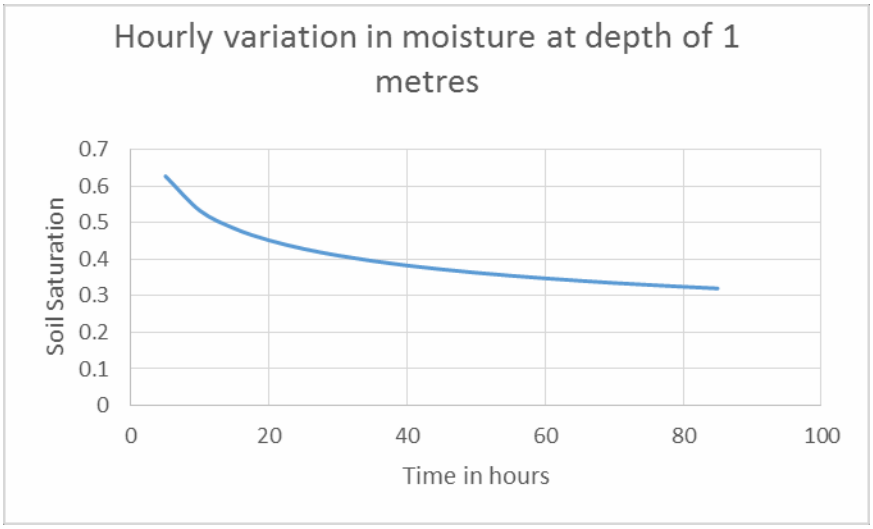


Fig 5.4: Hourly variation in moisture at depth 1 meter in sample for case 1

**Case 2: Water table at 3 m depth.**

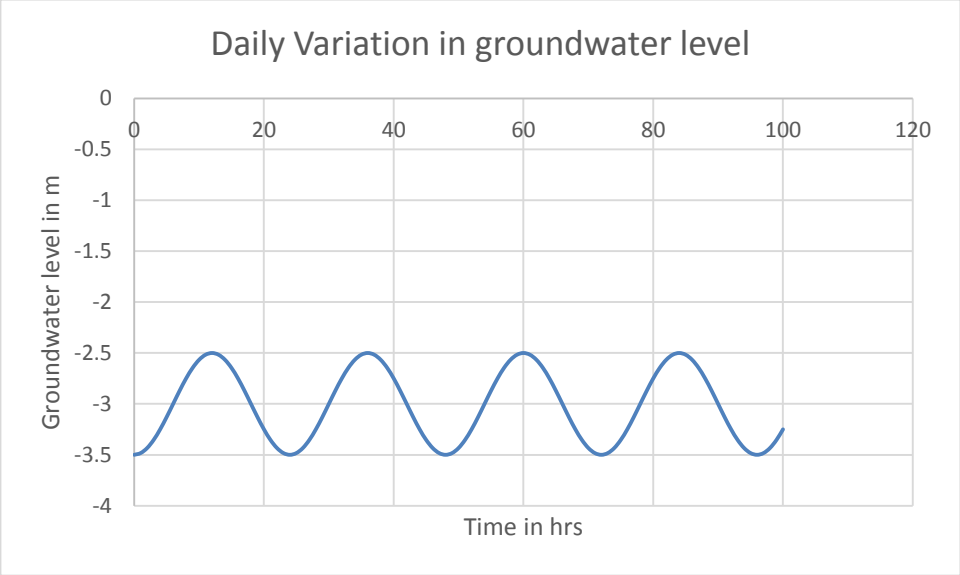


Fig 5.5: Daily variation in groundwater level at depth of 3.5 m.

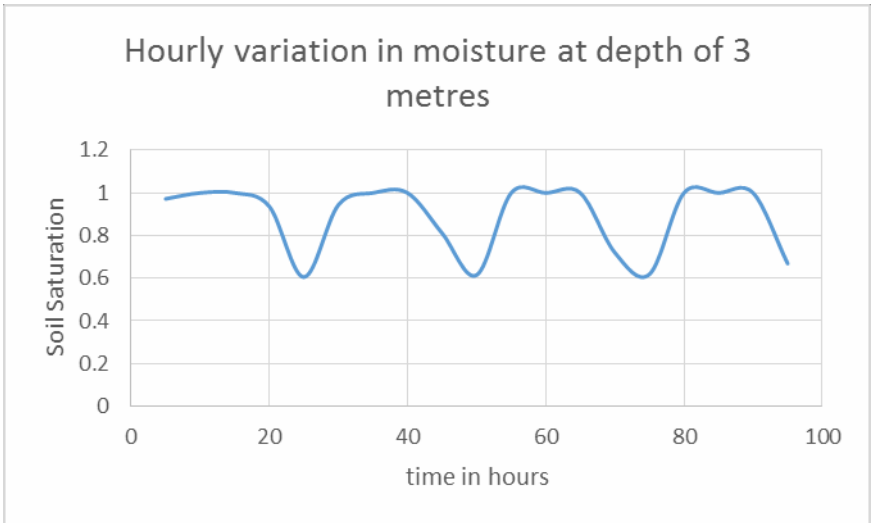


Fig 5.6: Hourly variation in moisture at depth 3 meter in sample for case 2.

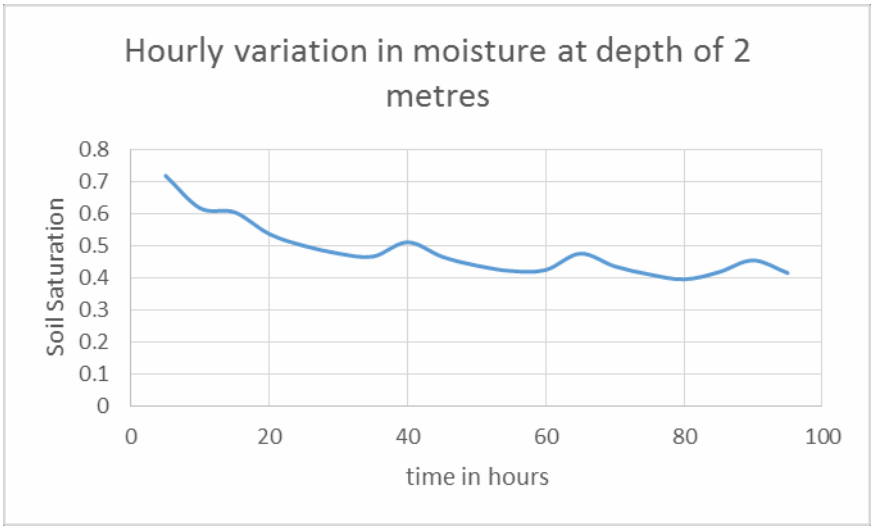


Fig 5.7: Hourly variation in moisture at depth 2 meter in sample for case 2.

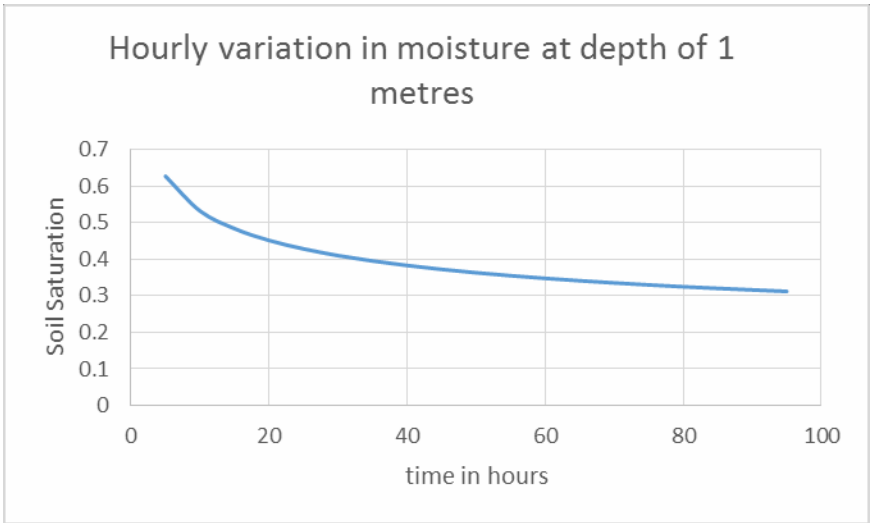


Fig 5.8: Hourly variation in moisture at depth 1 meter in sample for case 2.

**Case 3: Water table at 2 m depth.**

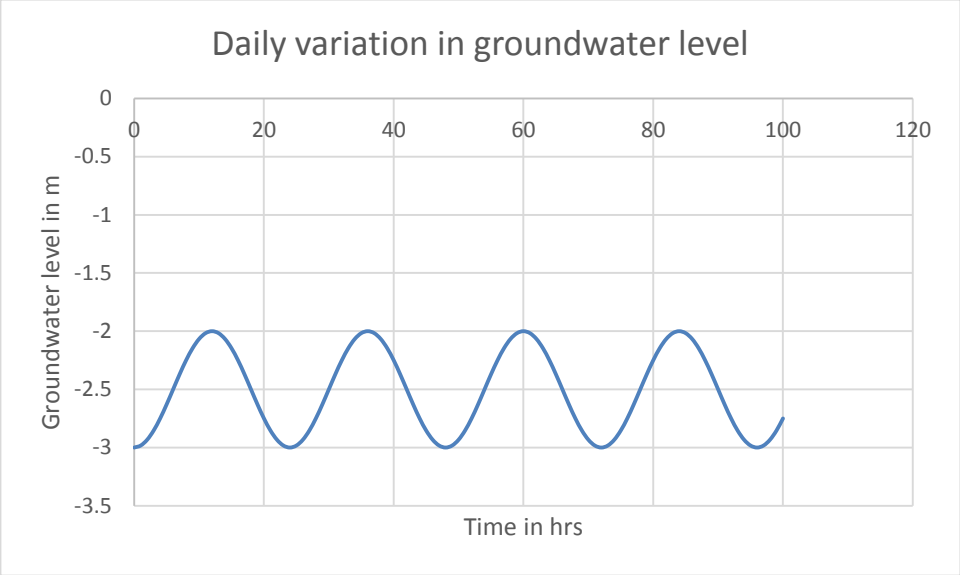


Fig 5.9: Daily variation in groundwater level at depth of 2 m.

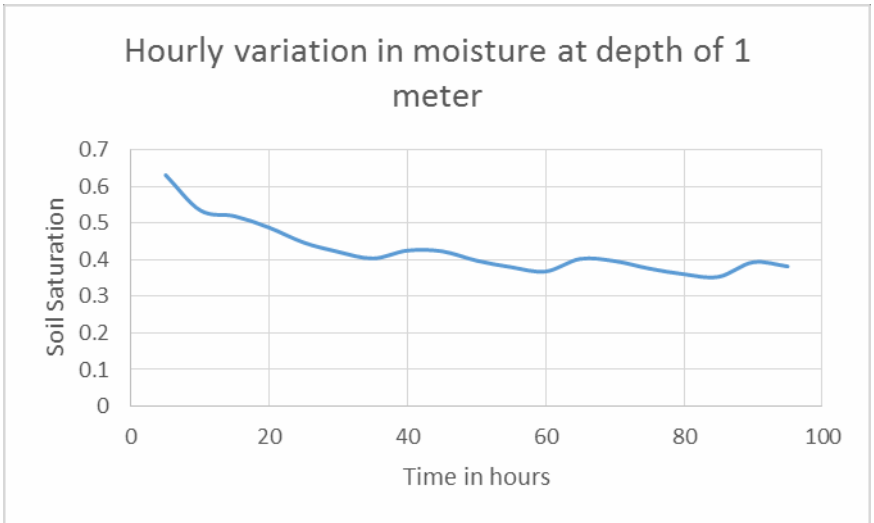


Fig 5.10: Hourly variation in moisture at depth 1 meter in sample for case 3

**WEEKLY VARIATION:**

**Case 1: Water table at 3.5 m depth from the top.**

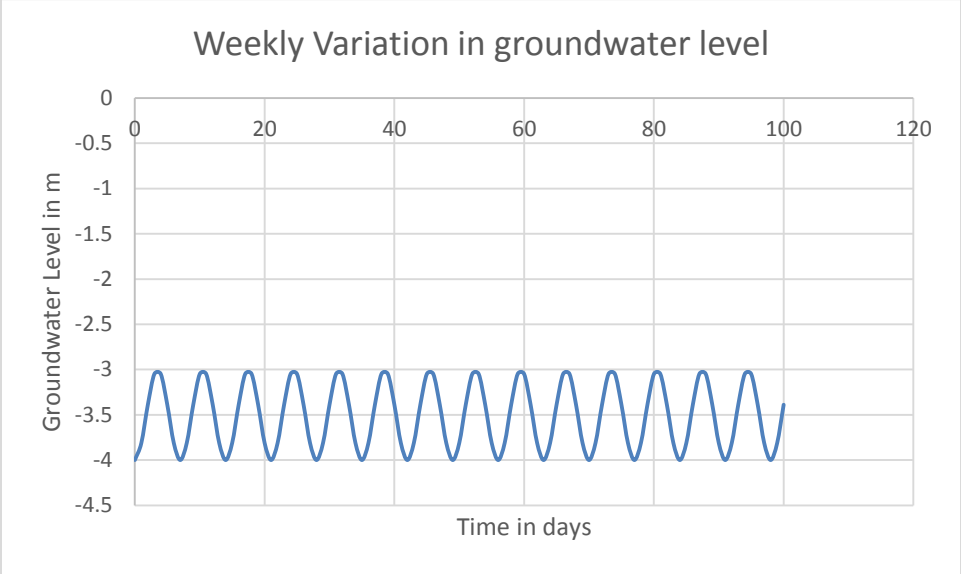


Fig 5.11: Weekly Variation in groundwater level at depth 3.5 m.

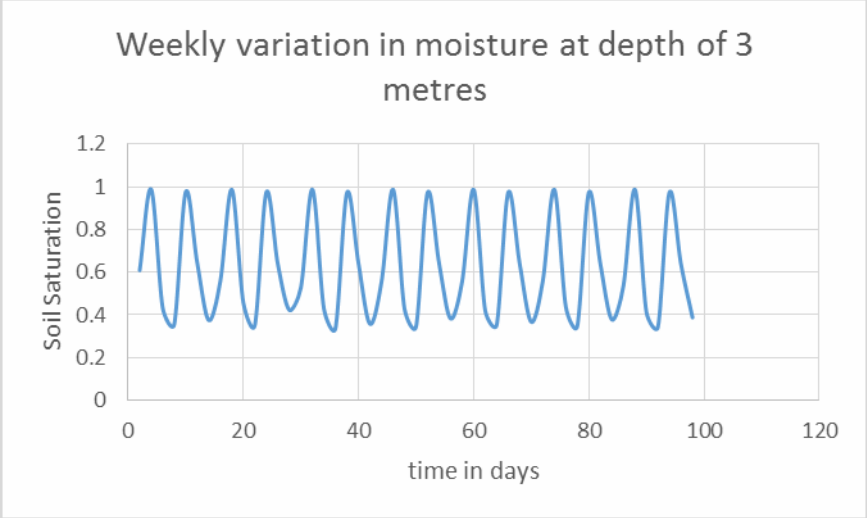


Fig 5.12: weekly variation in moisture at depth 1 meter in sample for case 1

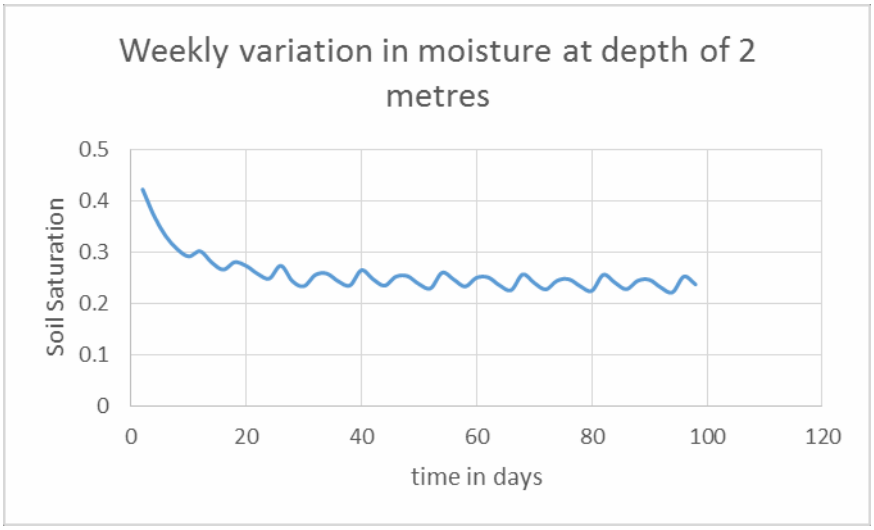


Fig 5.13: weekly variation in moisture at depth 2 meter in sample for case 1

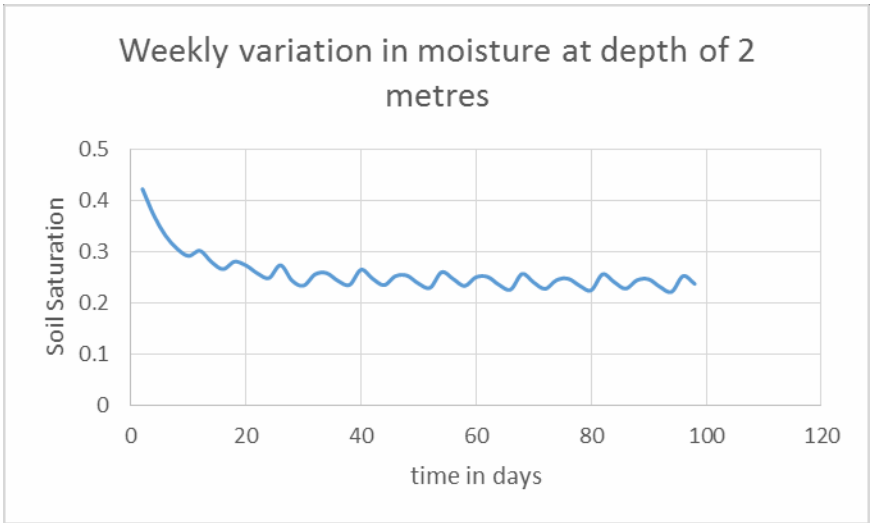


Fig 5.14: weekly variation in moisture at depth 1 meter in sample for case 1

**Case 2: Water table at 3 m depth from the top.**

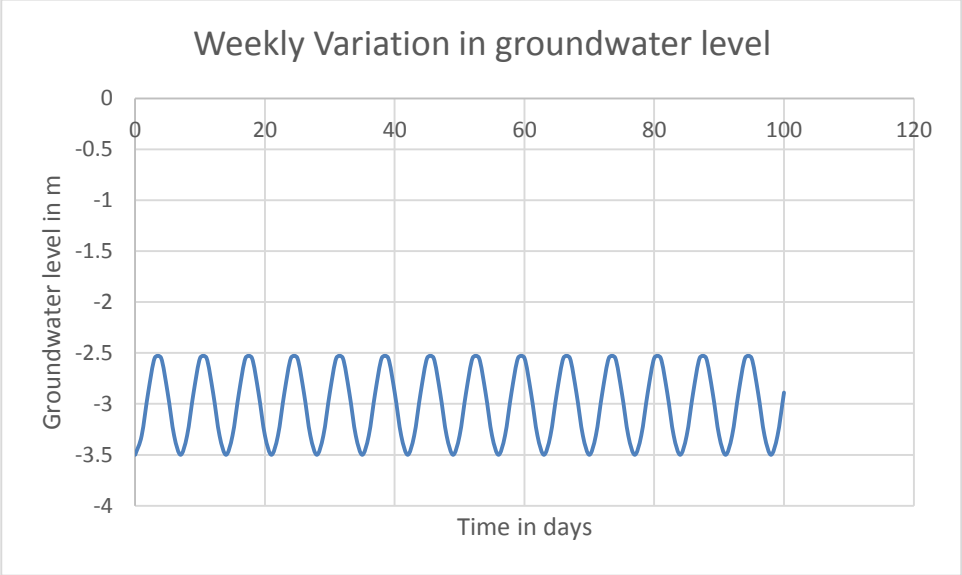


Fig 5.15: Weekly variation in groundwater level at 3 m depth.

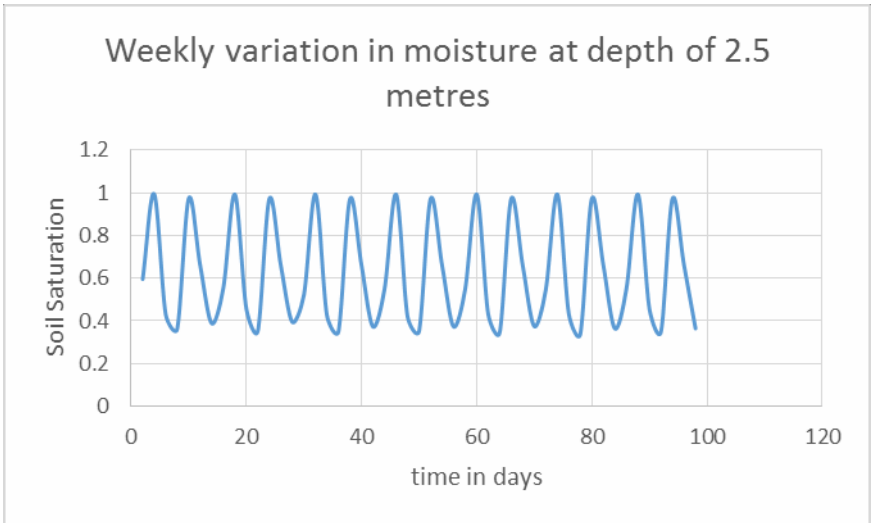


Fig 5.16: weekly variation in moisture at depth 2.5 meter in sample for case 2

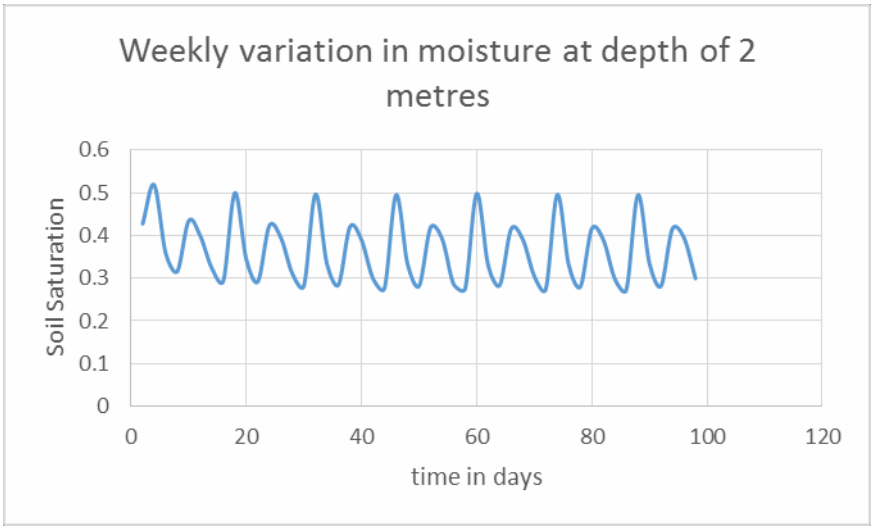


Fig 5.17: weekly variation in moisture at depth 2 meter in sample for case 2

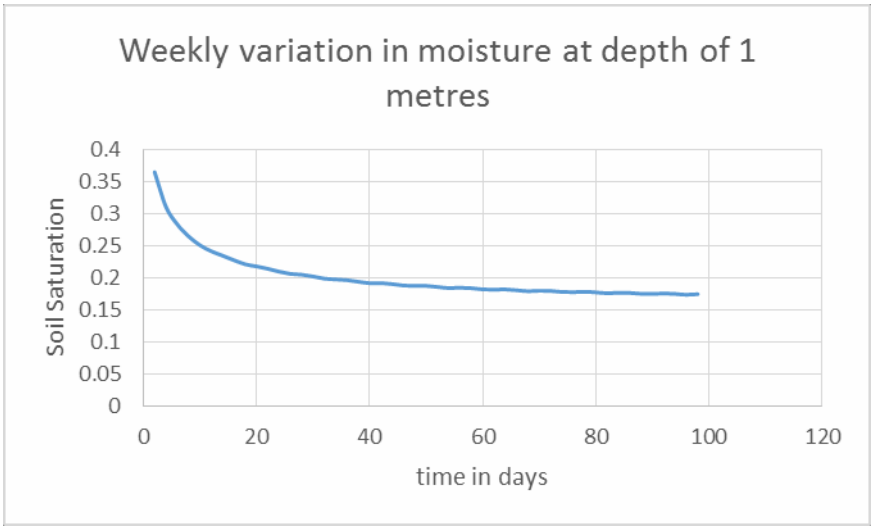


Fig 5.18: weekly variation in moisture at depth 1 meter in sample for case 2

**Case 3: Water table at 2 m depth from the top.**

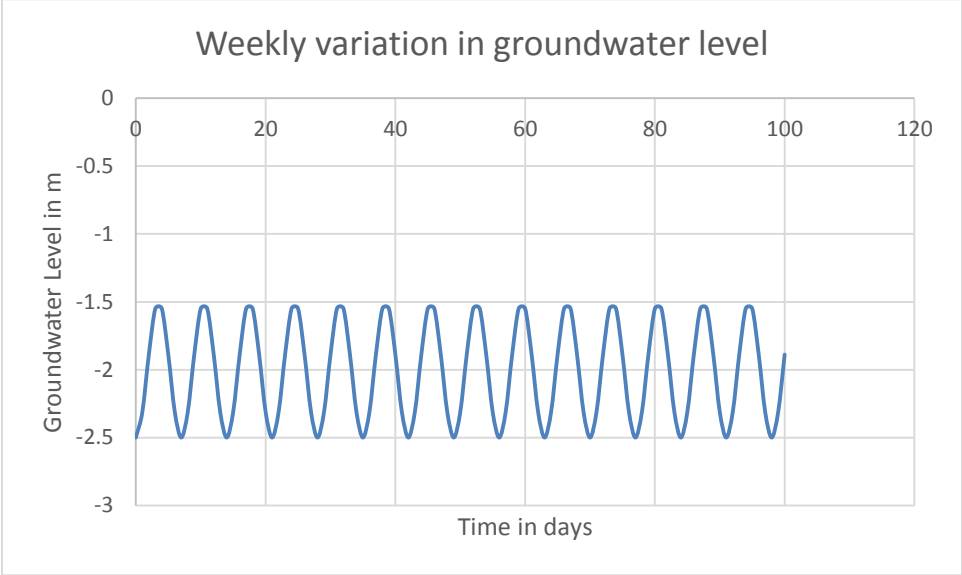


Fig 5.19: Weekly variation in groundwater level at depth 2 m

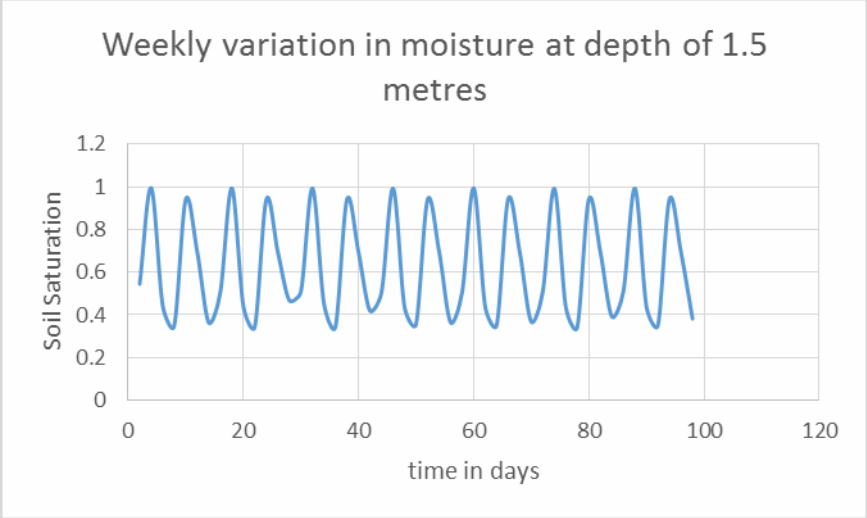


Fig 5.20: weekly variation in moisture at depth 1.5 meter in sample for case 3

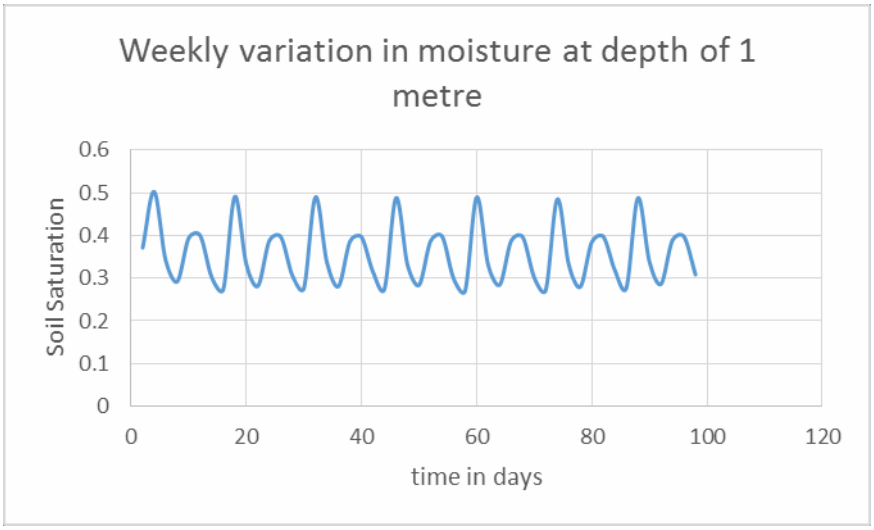


Fig 5.21: weekly variation in moisture at depth 1 meter in sample for case 3

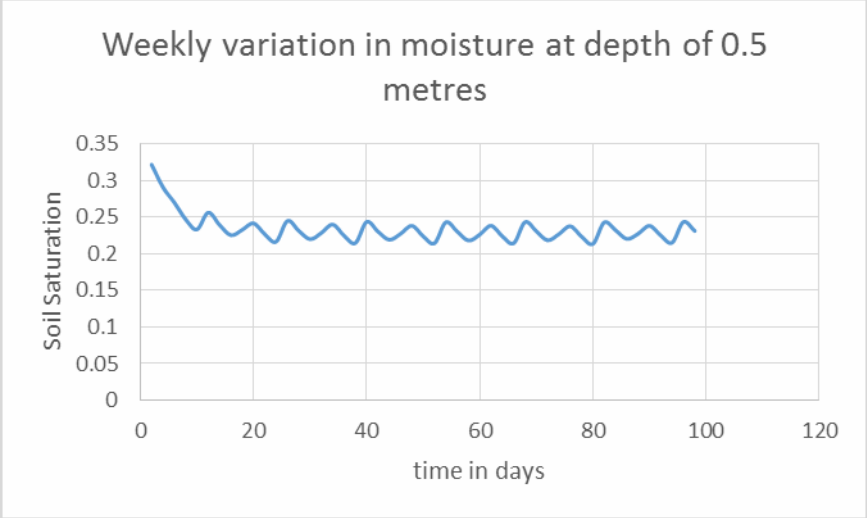


Fig 5.22: weekly variation in moisture at depth 0.5 meter in sample for case 3

**YEARLY VARIATION:**

**Case 1: Water table at 3.5 m depth from the top.**

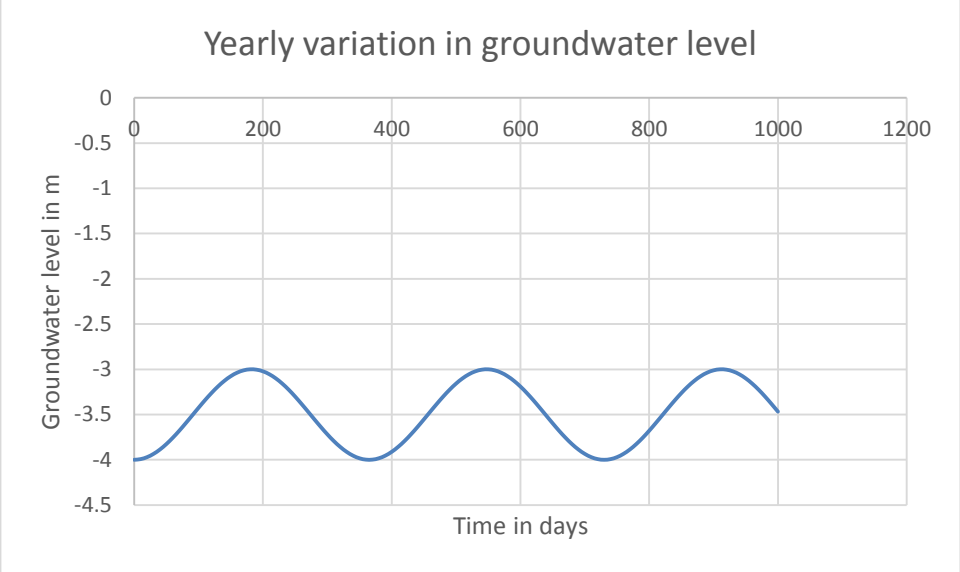


Fig 5.23: Yearly variation in groundwater level at depth 3.5 m

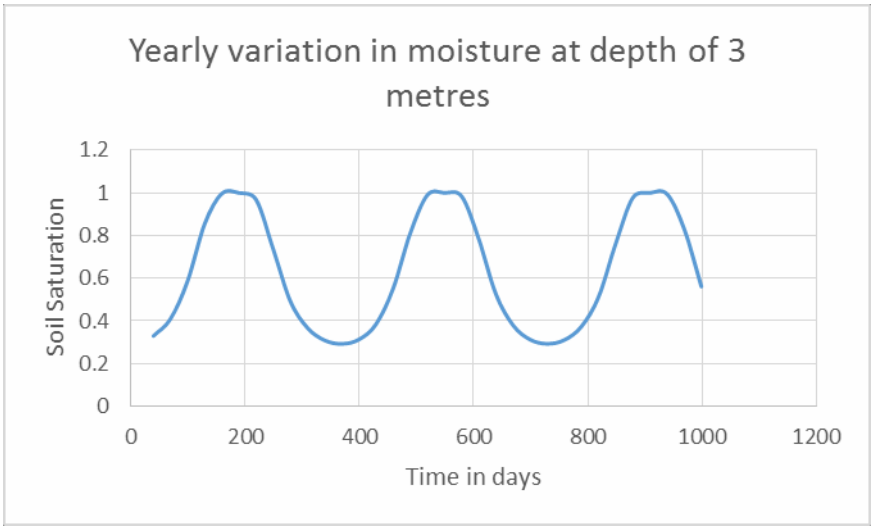


Fig 5.24: Yearly variation in moisture at depth 3 meter in sample for case 1

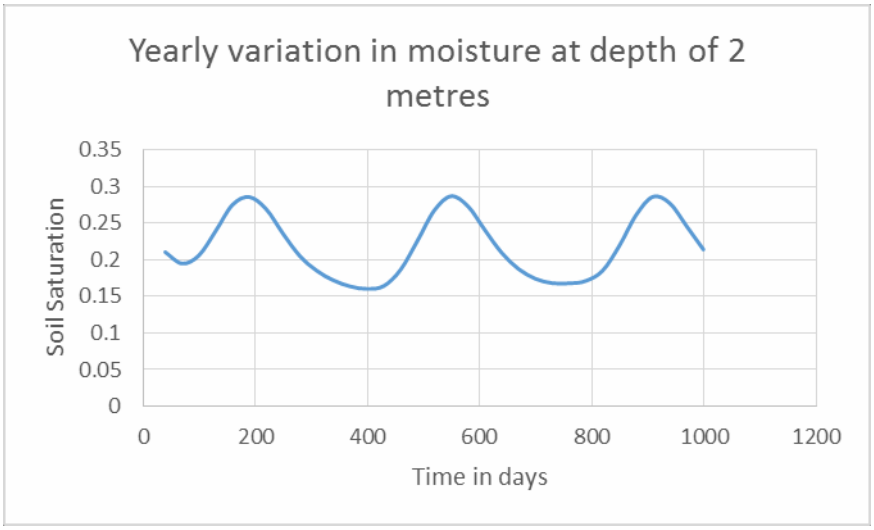


Fig 5.25: Yearly variation in moisture at depth 2 meter in sample for case 1

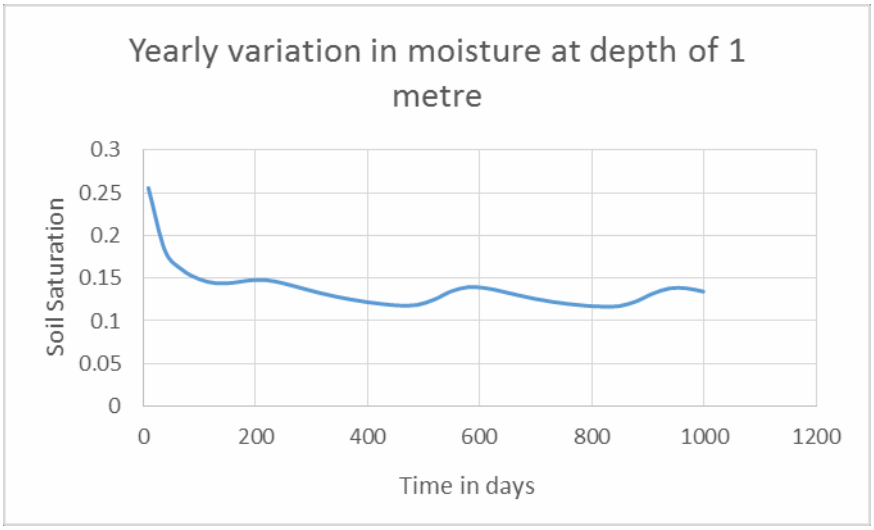


Fig 5.26: Yearly variation in moisture at depth 1 meter in sample for case 1

**Case 2: Water table at 3 m depth from the top.**

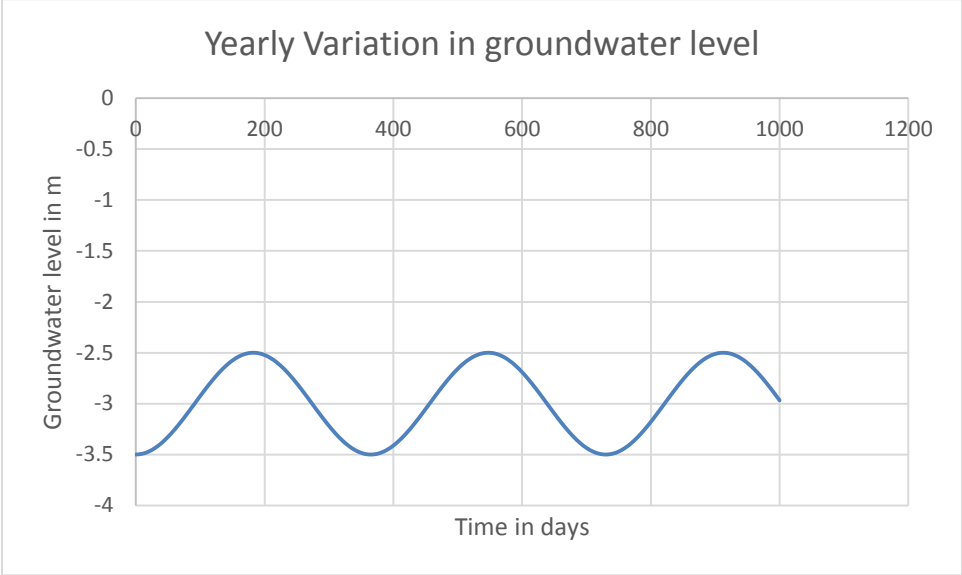


Fig 5.27: Yearly variation in groundwater level at depth 3 m

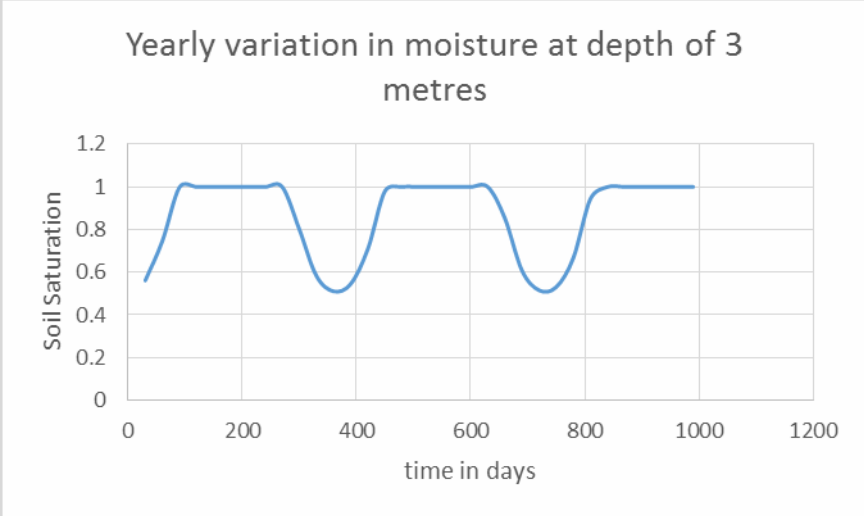


Fig 5.28: Yearly variation in moisture at depth 3 meter in sample for case 2

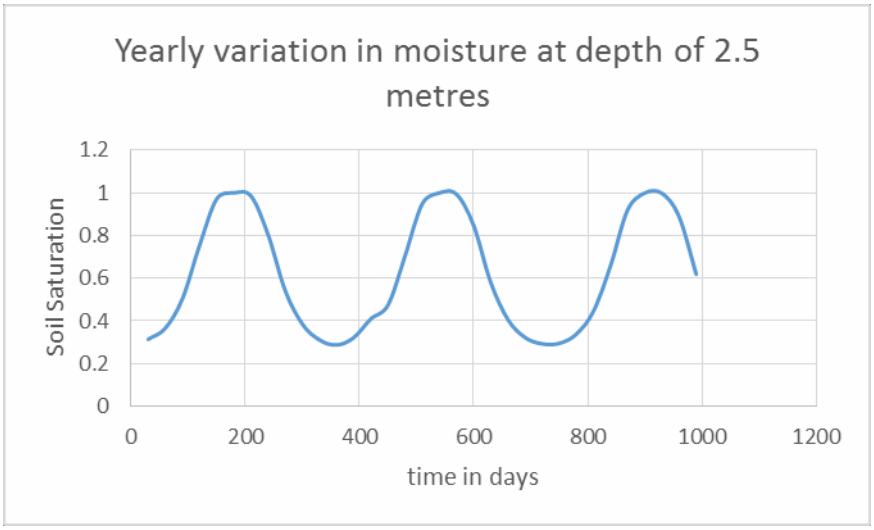


Fig 5.29: Yearly variation in moisture at depth 2.5 meter in sample for case 2

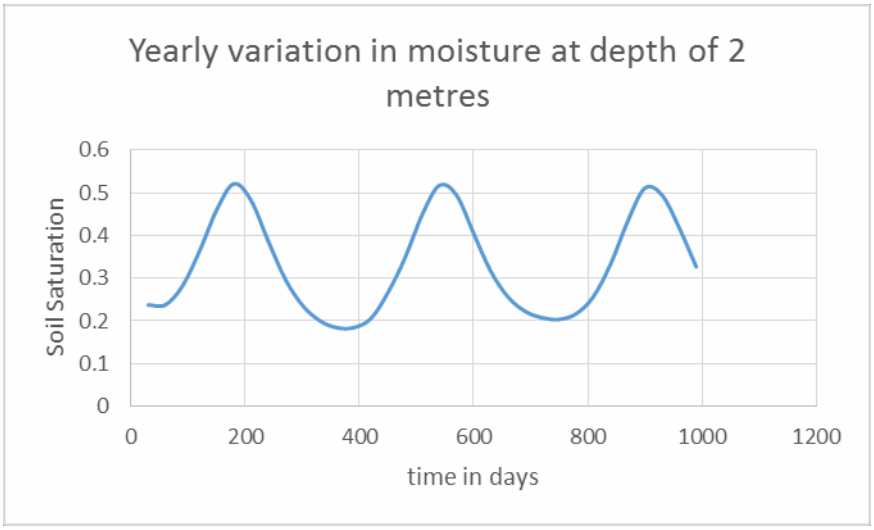


Fig 5.30: Yearly variation in moisture at depth 2 meter in sample for case 2

**Case 3: Water table at 2 m depth from the top.**

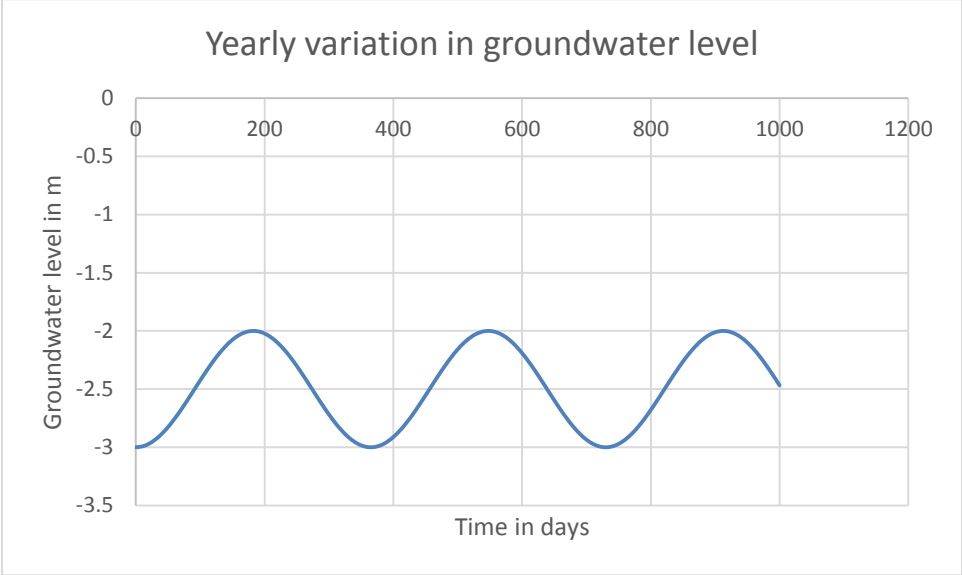


Fig 5.31: Yearly variation in groundwater level at depth 2 m.

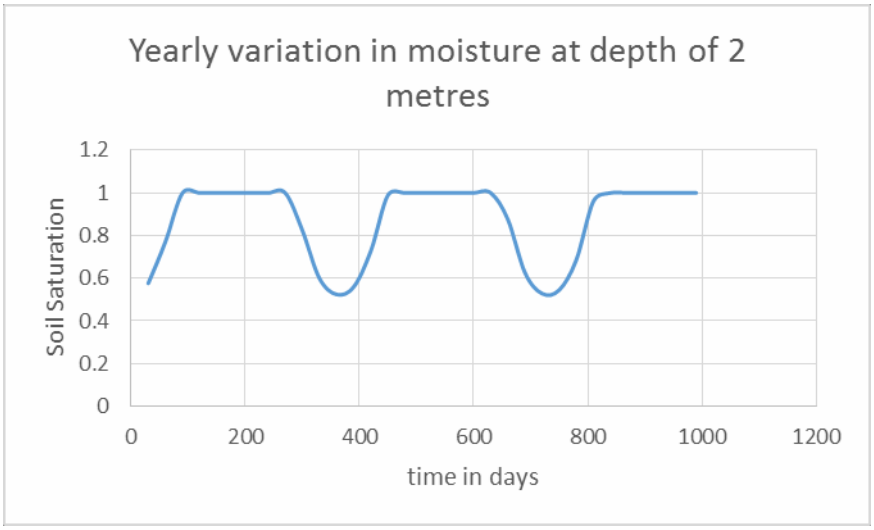


Fig 5.32: Yearly variation in moisture at depth 2 meter in sample for case 3

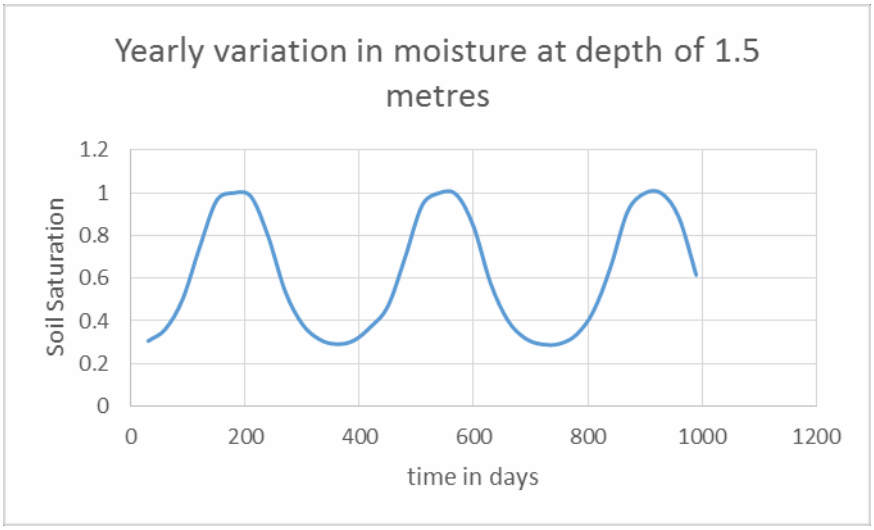


Fig 5.33: Yearly variation in moisture at depth 1.5 meter in sample for case 3

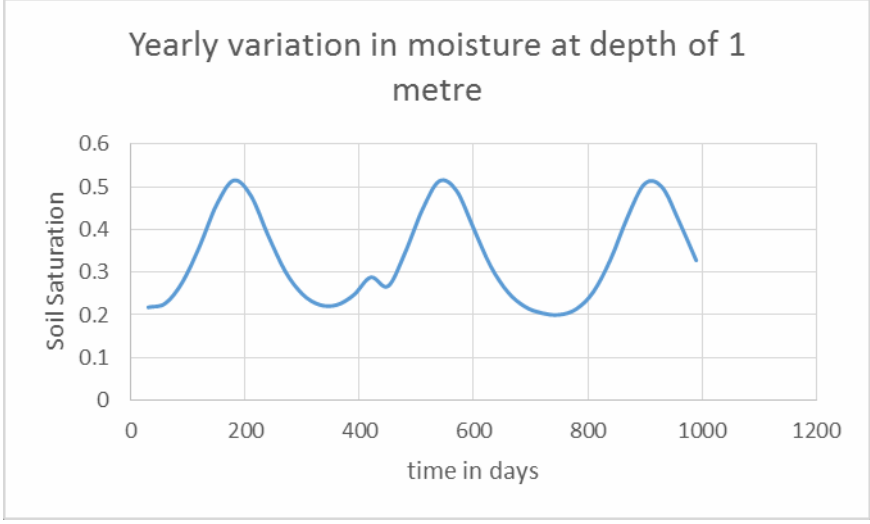


Fig 5.34: Yearly variation in moisture at depth 1 meter in sample for case 3

The figures 5.1, 5.5, 5.9, 5.11, 5.15, 5.19, 5.23, 5.27 and 5.31 show the change in groundwater table levels over the course of time. This variation is achieved, due to the variation in pressure head by using the equation 3.2, 3.3 and 3.4.

The soil moisture profiles for sand show a similar pattern over time for every time interval considered as seen in figures for soil moisture variation over various time durations. The graphs follow a similar path, with a gradual decrease in moisture content as the depth reduces or as the distance from the groundwater surface increases. However, as is seen in figures, the decrease in moisture content for yearly profiles is more significant than that over diurnal or weekly profile. The water content reduces to very low levels over the course of an year, achieving levels below 10% saturation, while the moisture content remains about 30 to 40% for weekly or daily profiles.

The soil moisture variation profiles for the sand sample, unlike the moisture profiles vary significantly in shape as well as amplitude for the various temporal variations.

The soil moisture variation profile for yearly variation shows the most well defined sinusoidal wave patterns as seen in figures **5.24, 5.25, 5.26, 5.28, 5.29, 5.30, 5.32, 5.33, 5.34.** The profiles are clearer and more pronounced at depths closer to the water table. As we move away from the water table as in figure **5.26**, the soil moisture profile is not as well defined. This may be attributed to the fact that as the moisture level reduces, the change in moisture content gets less significant and it becomes almost similar.

As the yearly variation profiles were drawn over a total time period of 1000 days, two (2) full cycles and one (1) partial cycle can be observed.

The soil moisture profile for weekly variation also shows a well developed sinusoidal wave pattern over depths closer to the groundwater table. The figures **5.12, 5.13, 5.14, 5.16, 5.17, 5.18, 5.20, 5.21, 5.22** show the soil moisture variation profiles for sand over

weekly intervals for various depths. The soil moisture profile in fig **5.12, 5.16 and 5.20** show the best defined sinusoidal patterns. As this profile is drawn over a 100 day period, there are 14 fully developed cycles of the soil moisture variation. Similar to the yearly profiles, the weekly profiles are also lesser defined as the depth reduces or as we move away from the groundwater table surface.

The diurnal profiles for soil moisture variation are shown in fig **5.2, 5.3, 5.4, 5.6, 5.7, 5.8, 5.10**. These profiles are not as well developed as those of weekly and yearly time intervals. This may be attributed to the fact that the soil moisture has lesser time to be able to generate well defined patterns. The diurnal profiles were studied over 100 hours, which meant 4 complete cycles and one incomplete one.

As seen in the profiles for all three time intervals, the moisture variation profile is well defined at depths closer to the groundwater surface. The maximum saturation is almost 100% in such profiles. As we move away from the water table surface, the maximum saturation levels are lesser and the sinusoidal diagrams are lesser pronounced. This may be due to the ease in transport of groundwater over smaller vertical distances. That is not the case for depths of 1 meter or 2 meters. This may be attributed to the fact that more capillary forces are required for the transport of groundwater over such distances from the water table.

## For Gravel:

For plotting the temporal variation of moisture in a model of gravel, the following values of hydraulic components were considered:

$K_s = 3 \times 10^{-3}$ m/d

$\Theta_s = 0.5$

$\alpha = 20$ /m

$n = 4$

The temporal variation was done on diurnal and yearly levels. While the soil profile shapes remain similar, there is a change in the top soil saturation levels for each case.

**Yearly Variation:**

**Case 1: water table at 3 m from top**

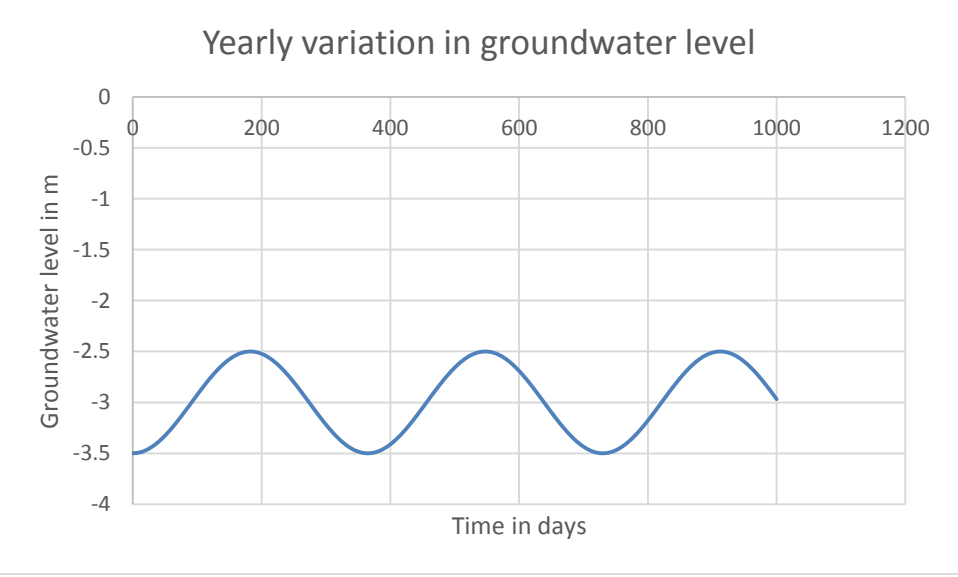


Fig 5.35: Yearly Variation in groundwater level at depth 3 m.

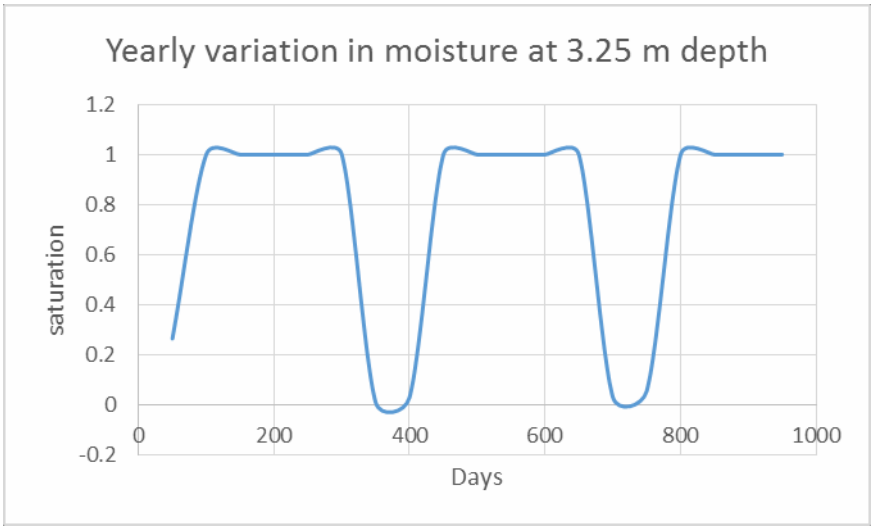


Fig 5.36: Yearly variation in moisture at depth 3.25 meter in sample for case 1

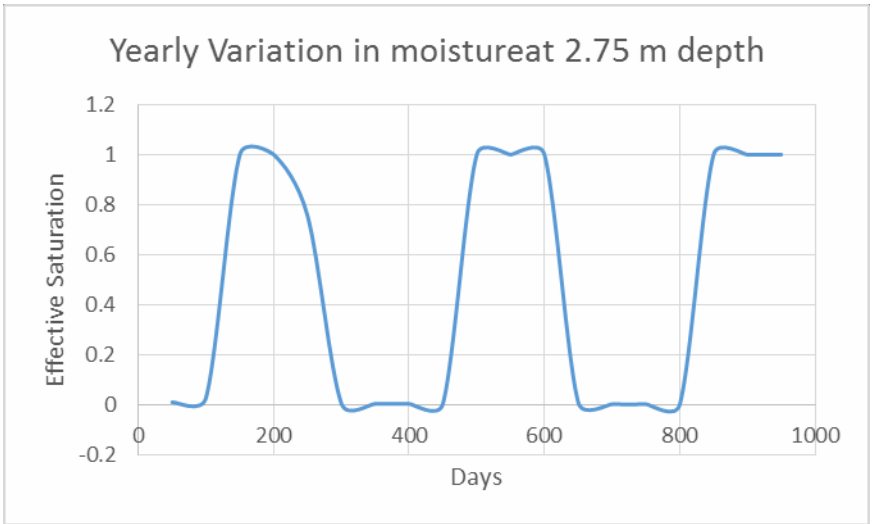


Fig 5.37: Yearly variation in moisture at depth 2.75 meter in sample for case 1

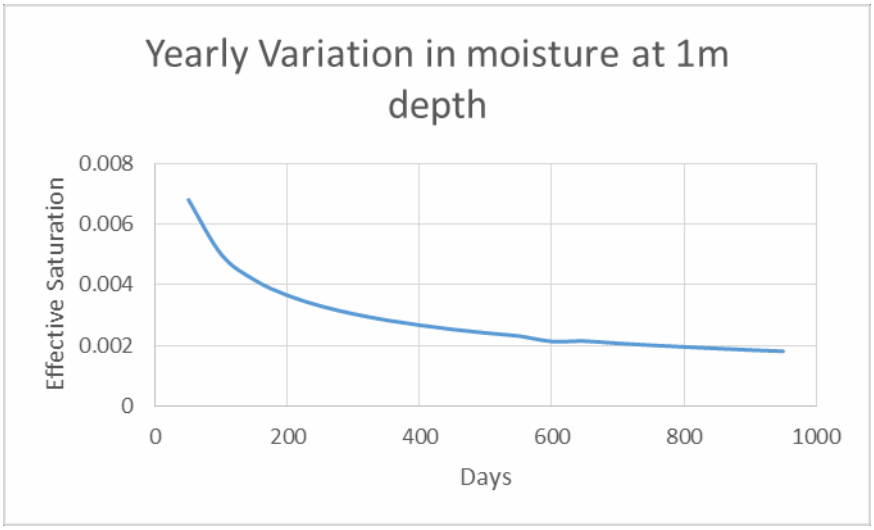


Fig 5.38: Yearly variation in moisture at depth 1 meter in sample for case 1

**Case 2 : Water table at 2 m from top**

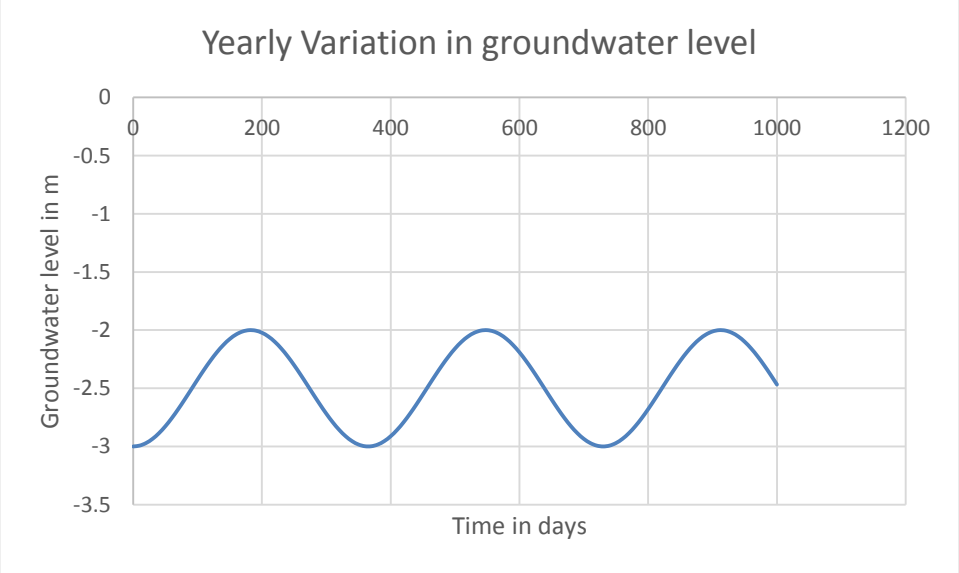


Fig 5.39: Yearly variation in Groundwater level at depth of 2 m

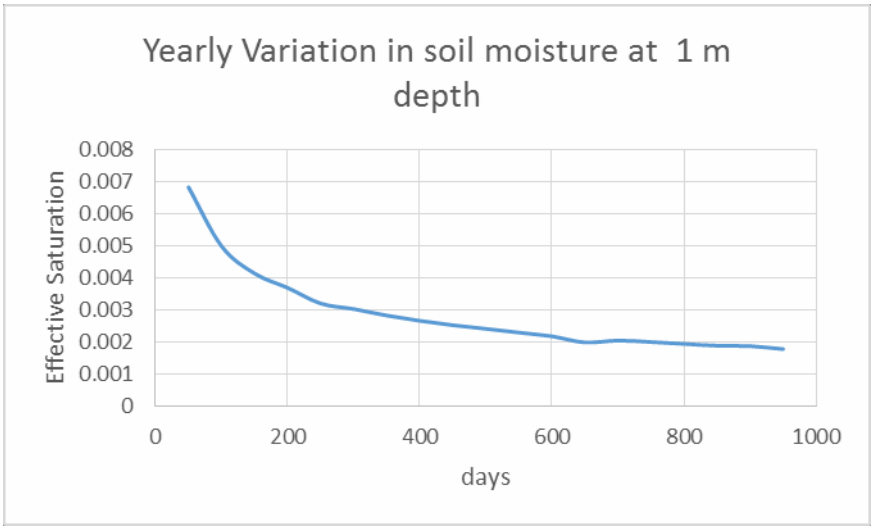


Fig 5.40: Yearly variation in moisture at depth 1 meter in sample for case 2

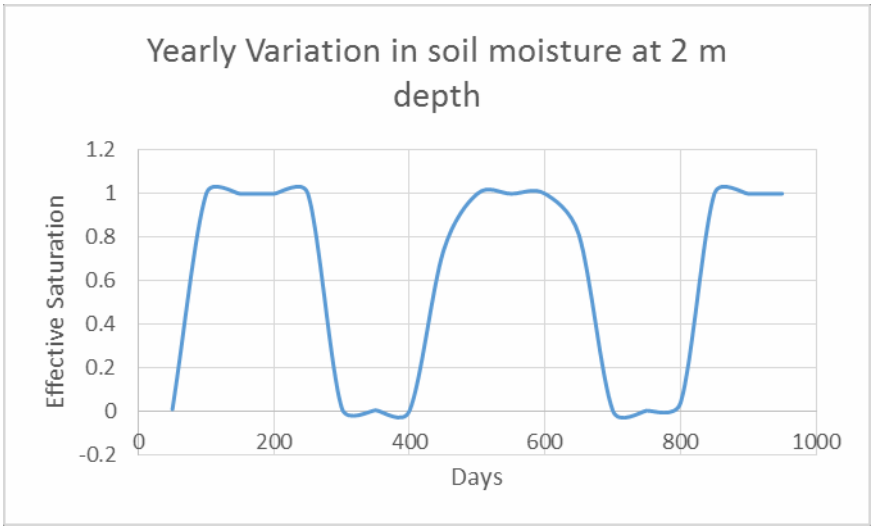


Fig 5.41: Yearly variation in moisture at depth 2 meter in sample for case 2

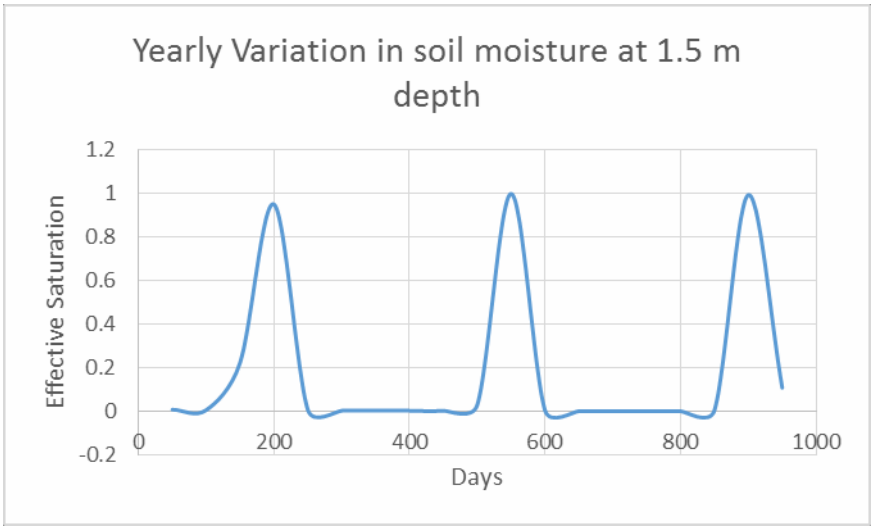


Fig 5.42: Yearly variation in moisture at depth 1.5 meter in sample for case 2

**Case 3: Water table at 2.5 m from top**

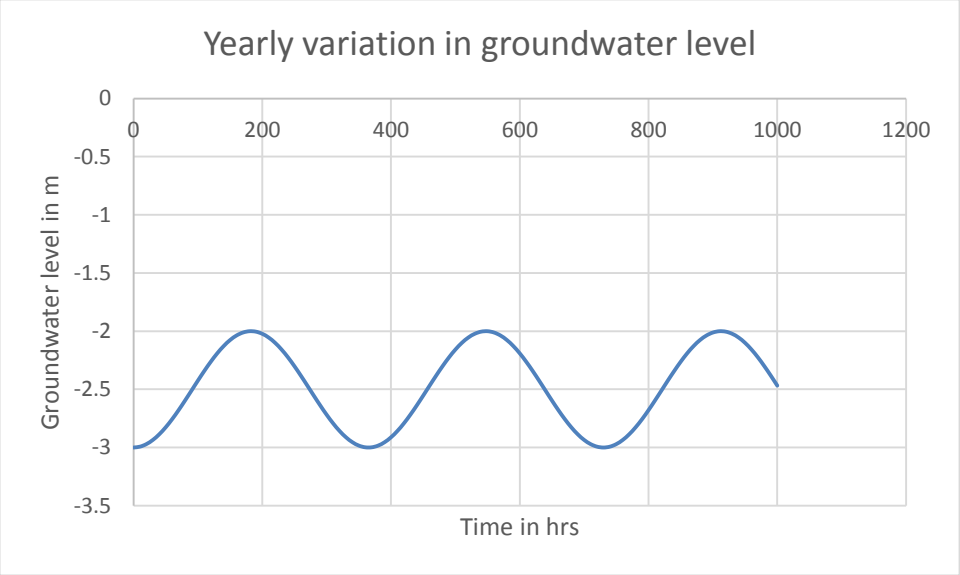


Fig 5.43: Yearly Variation in groundwater level at depth 2.5 m

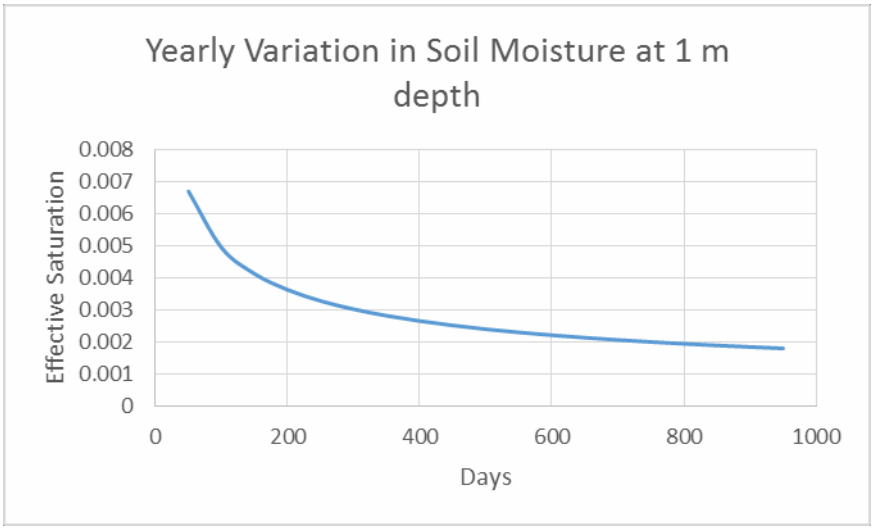


Fig 5.44: Yearly variation in moisture at depth 1 meter in sample for case 3

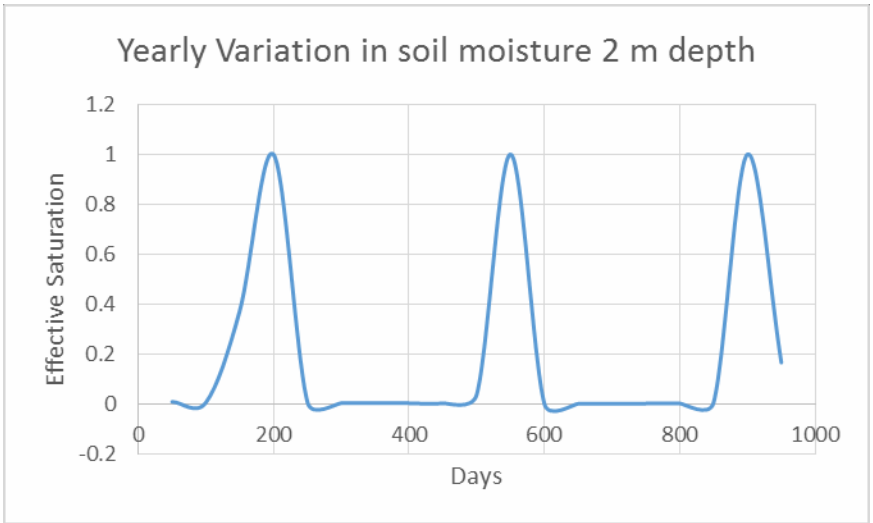


Fig 5.45: Yearly variation in moisture at depth 2 meter in sample for case 3

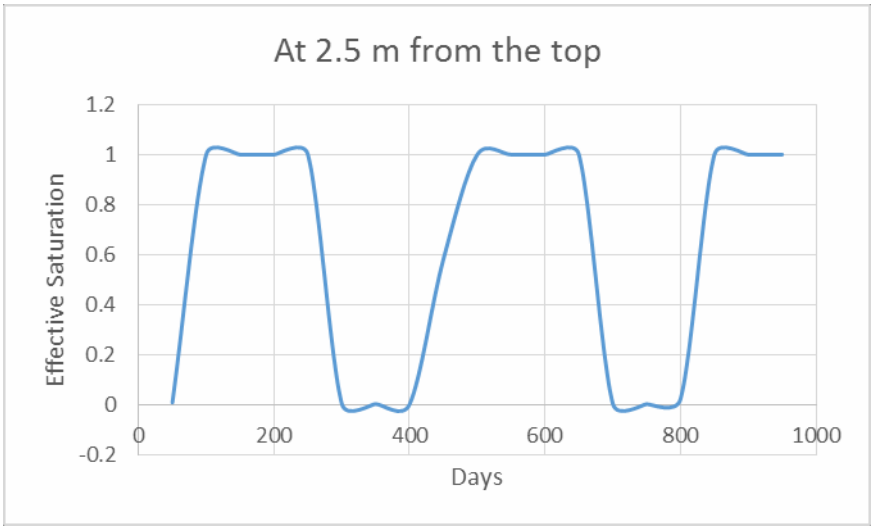


Fig 5.46: Yearly variation in moisture at depth 2.5 meter in sample for case 3

**Diurnal Variation in Soil Moisture:**

**Case 1: Water table at 3 m from top:**

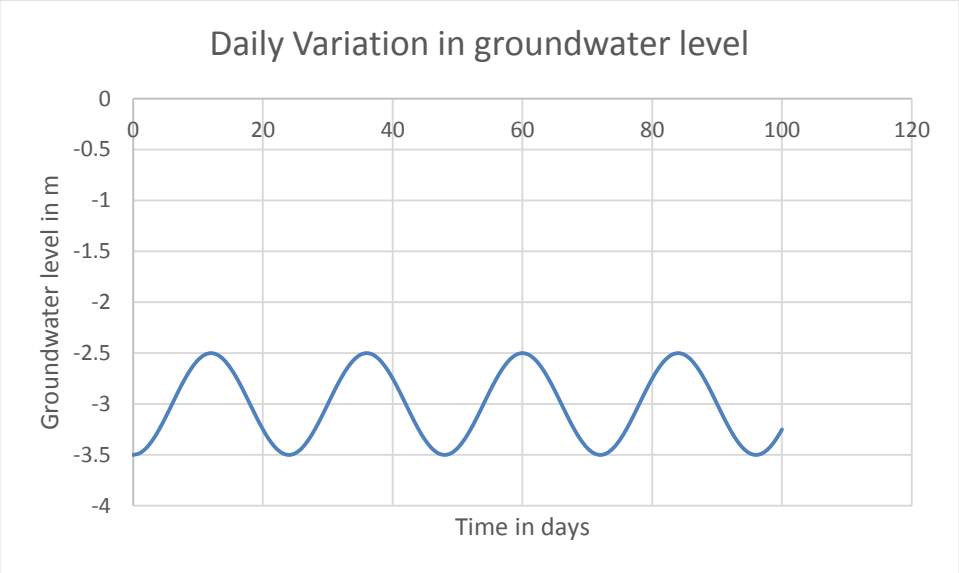


Fig 5.47: Daily Variation in groundwater level at depth 3 m

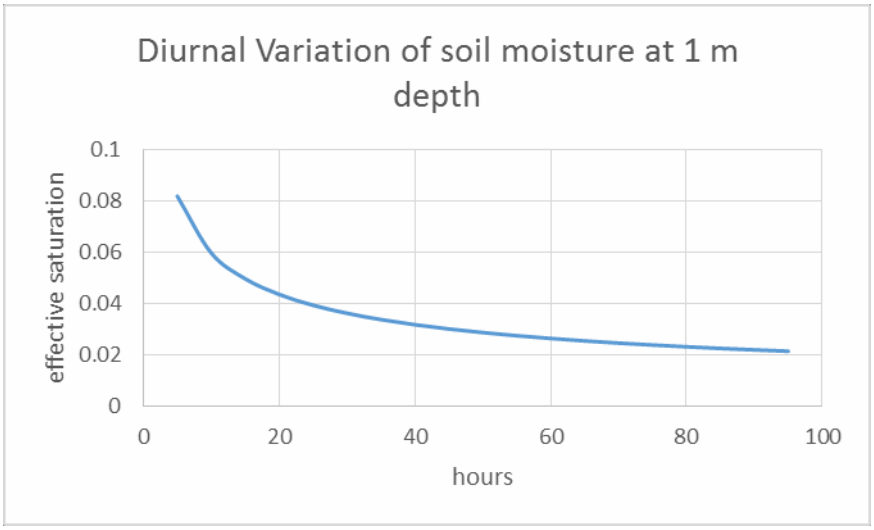


Fig 5.48: Daily variation in moisture at depth 1 meter in sample for case 1

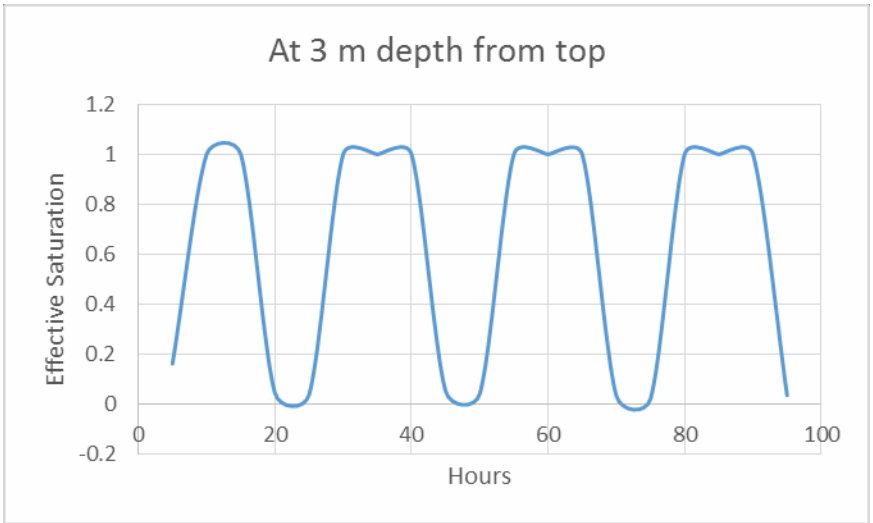


Fig 5.49: Daily variation in moisture at depth 3 meter in sample for case 1

**Case 2 : Water table at 2 m from top:**

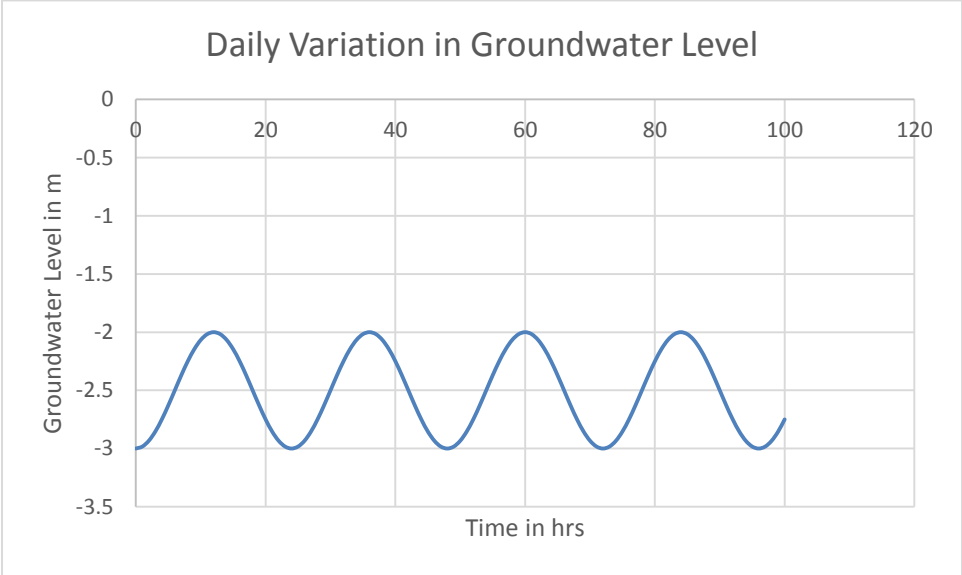


Fig 5.50: Daily Variation in Groundwater Level at depth 2 m

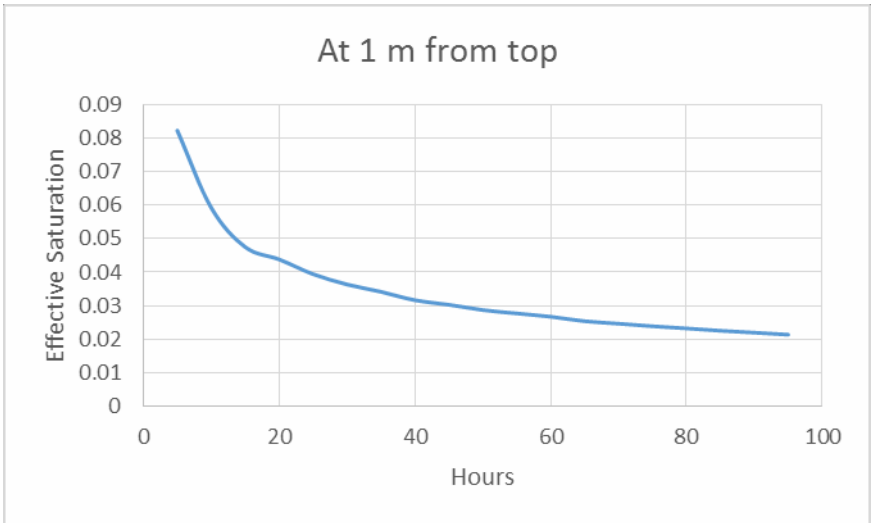


Fig 5.51: Daily variation in moisture at depth 1 meter in sample for case 2

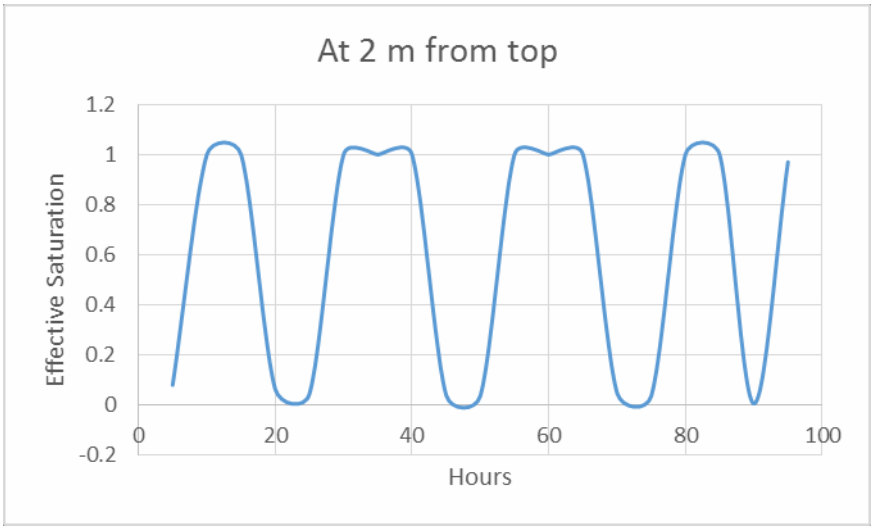


Fig 5.52: Daily variation in moisture at depth 2 meter in sample for case 2

**Case 3: Water table at 2.5 m from top:**

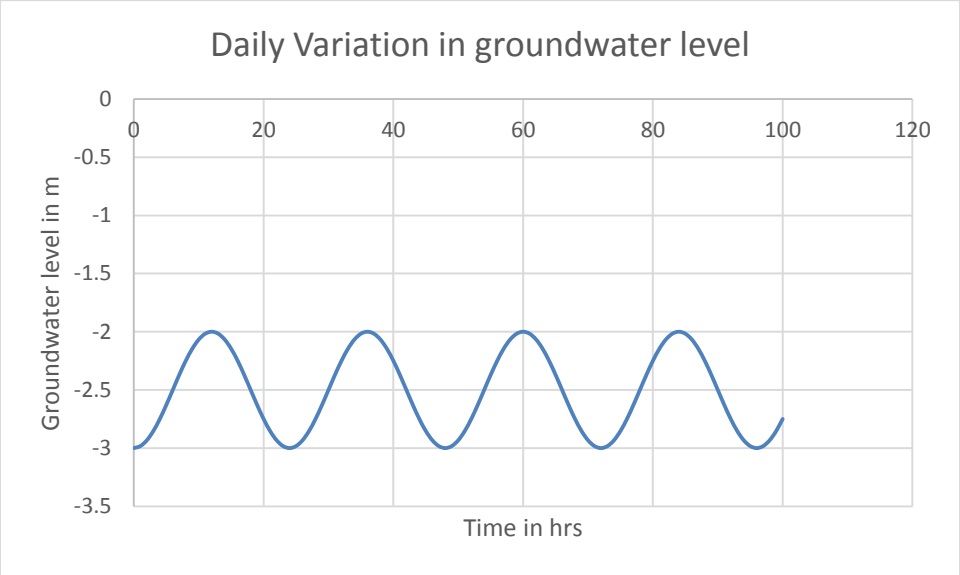


Fig 5.53: Daily Variation in groundwater level at depth 2.5 m

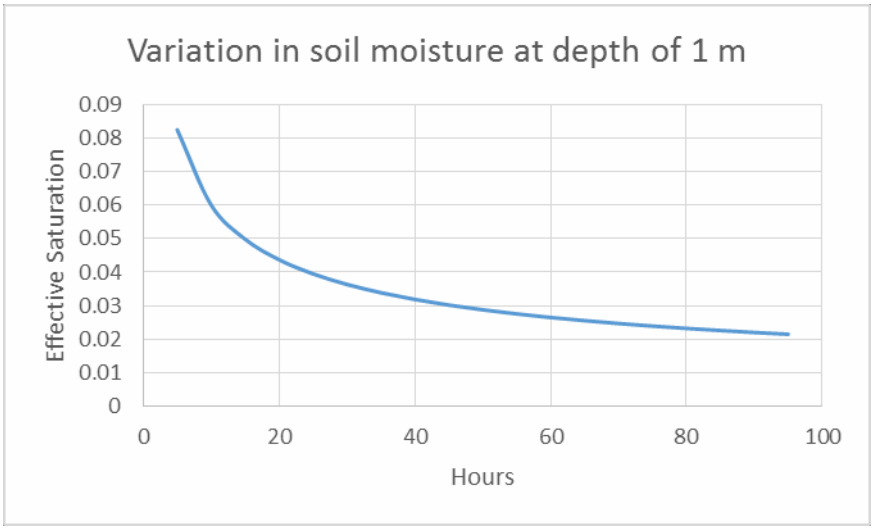


Fig 5.54: Daily variation in moisture at depth 1 meter in sample for case 3

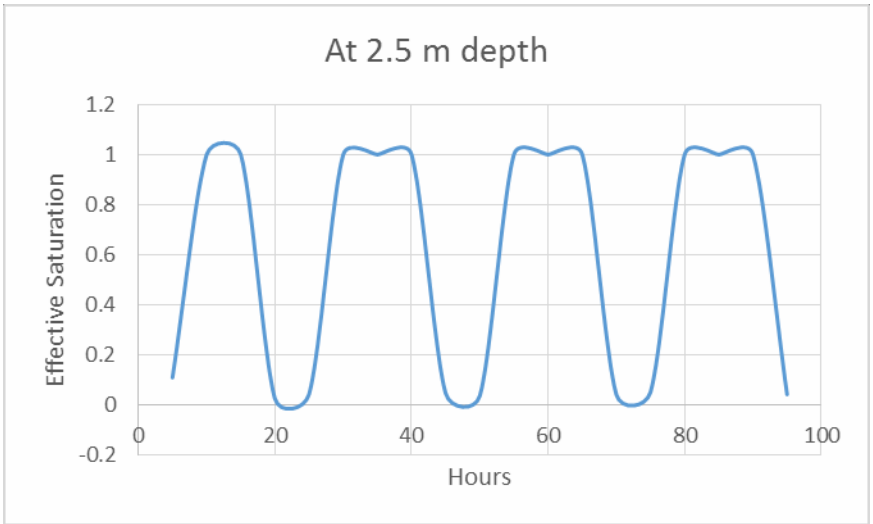


Fig 5.55: Daily variation in moisture at depth 2.5 meter in sample for case 3

The figures 5.35, 5.39, 5.43, 5.471, 5.50 and 5.53 show the change in groundwater table levels over the course of time. This variation is achieved, due to the variation in pressure head by using the equation 3.2, 3.3 and 3.4.

The soil moisture profile for gravel is noticeably different from that of sand. The large porosity reduces the capillarity effect of the soil to a minimum. Hence, as seen in Fig for moisture change, the change in moisture level is sharp, sudden and immediately above the water table.

The soil moisture variation profiles however, show similar traits to the ones for sand. As seen in the variation profiles for sand, sinusoidal profiles are observed at depths near to the water table. This is observed in **fig 5.36, 5.37, 5.41, 5.42, 5.45, 5.46, 5.49, 5.52, and 5.55.** The graphs vary sinusoidally with crests at 1 and troughs at 0. This is similar to the profiles observed in sand.

As the yearly variation profiles were drawn over a total time period of 1000 days, two (2) full cycles and one (1) partial cycle can be observed. The diurnal profiles were studied over 100 hours, which meant 4 complete cycles and one incomplete one.

As seen in the profiles for all three time intervals, the moisture variation profile is well defined at depths closer to the groundwater surface. The maximum saturation is almost 100% in such profiles. As we move away from the water table surface, the maximum saturation levels are lesser and the sinusoidal diagrams are lesser pronounced. This may be due to the ease in transport of groundwater over smaller vertical distances. That is not the case for depths of 1 meter or 2 meters. This may be attributed to the fact that more capillary forces are required for the transport of groundwater over such distances from the water table.

## For Clay and Silt:

The same model was used to determine the rise of water in clay and silt soils, under the influence of a changing groundwater table.

In this case:

$K_s = 1 \times 10^{-8}$ m/s

$\Theta = 0.6$

$\alpha = 2$

n = 1.3

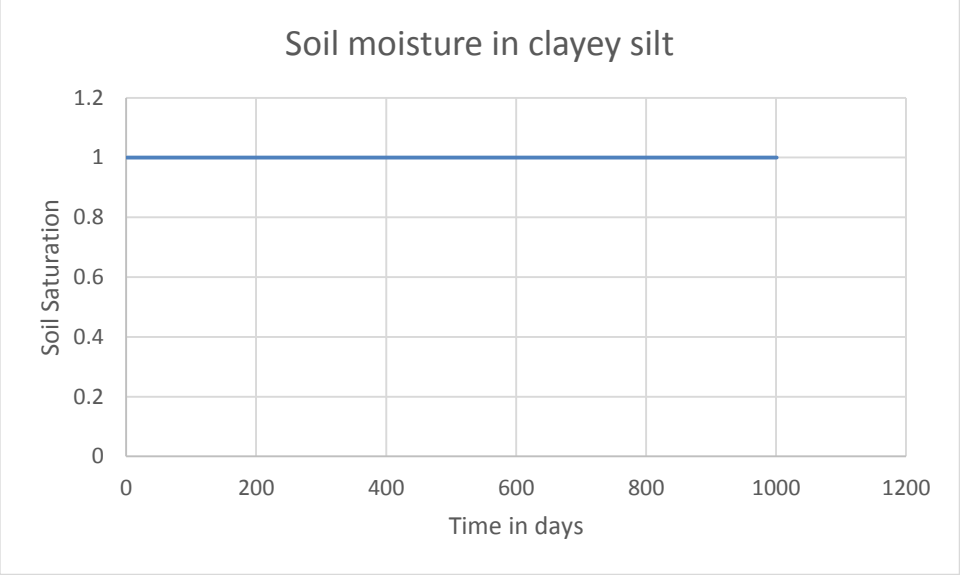


Fig 5.56: Yearly variation in moisture at depth 1 meter in sample for clayey silt

As seen, the capillary fringe is greater than the current model domain. Hence, the soil remains completely saturated in such a case. The capillary fringe was calculated for the given parameters, and was found to be 8 m.

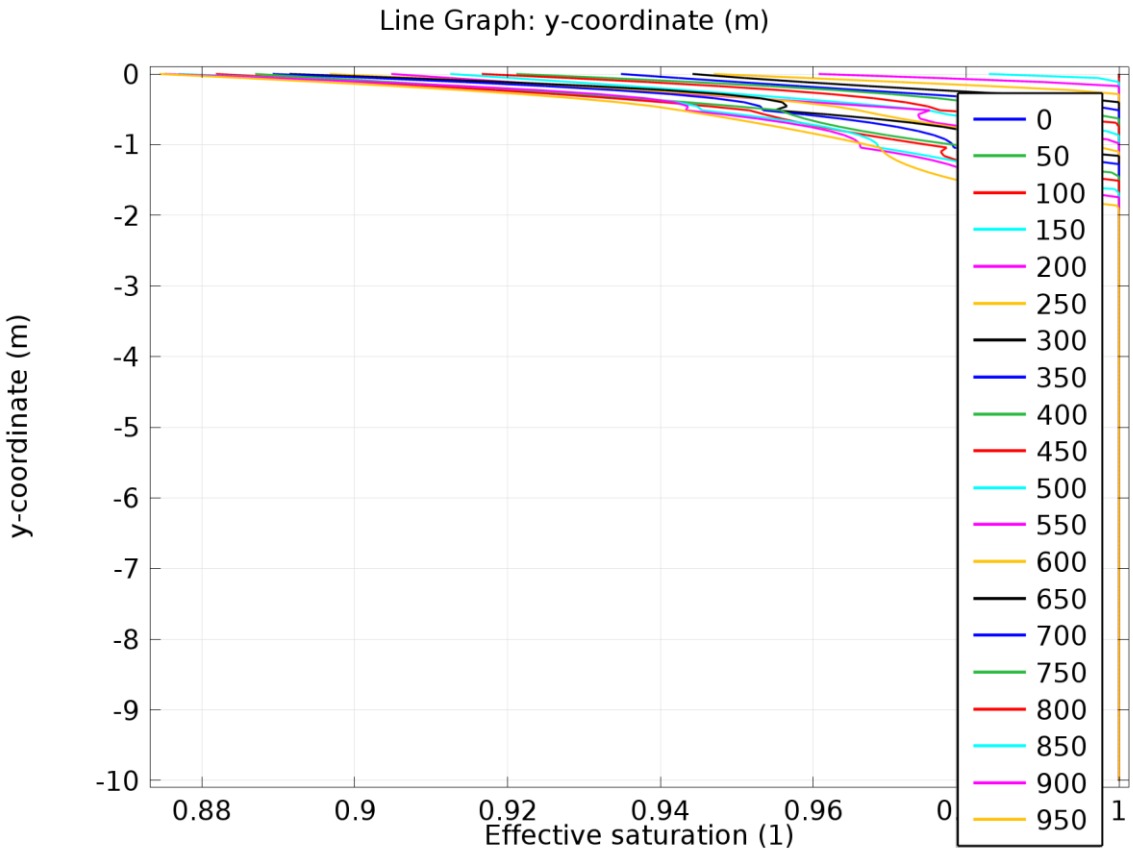


Fig 5.57: Variation in soil moisture content

As seen, the soil remains completely saturated till a depth of 2 m. Hence, it is not possible to plot the same on the current sample size of 4 m x 4 m.

The fig 5.57 shows a second model, which helps to find the capillary fringe of the soil. In this case, the height of the model taken is 10 m. The capillary fringe is found to be 8 m.

The higher capillarity or the thicker capillary fringe may be attributed to the smaller pore size of the clayey silt soil. The small pores help the adhesive forces between soil and water as well as the cohesive forces between the water molecules themselves to act on the water. Hence, the surface tension of water helps the water to climb up the small pores.

Steady State:

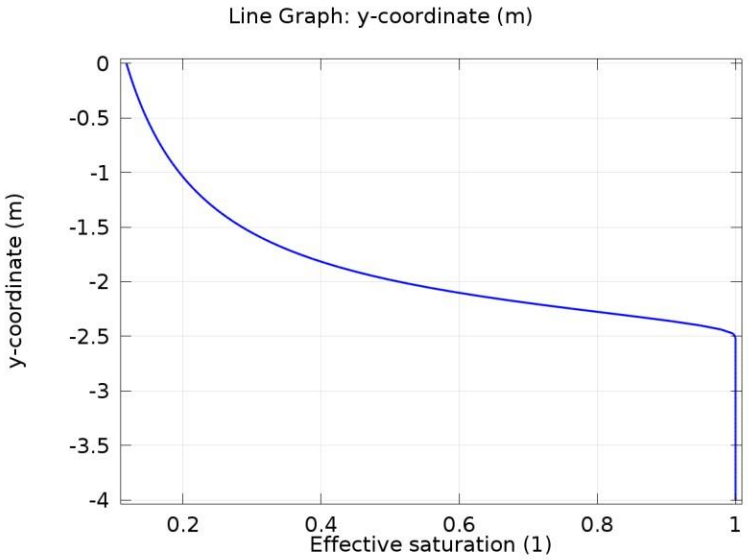


Fig 5.58: Moisture profile over the sample at steady state with the pressure head at 1.5 m

The soil moisture profile at steady state was plotted for sand with the pressure head constant at 1.5 m in fig **5.56**. The steady state profile is effective in showing the variation in profile over the soil sample. In other words, it helps to show the spatial variation in soil moisture. However, as seen, since there is no temporal variation in the pressure head, or any other parameter, the steady state condition cannot be used to study the variation in soil moisture in a soil sample with respect to time.

# CHAPTER 6

# CONCLUSIONS

1. The soil moisture profiles for the various soils show that the smaller the pore size, greater is the capillarity and hence, more water rises. In clay and silt, the moisture profiles show complete saturation throughout, while gravel has lesser moisture transport. Hence, crops such as rice and cotton are planted in clay, while millets needing less water are planted in gravelly and sandy soils.
2. The minimum soil moisture level for diurnal models is significantly higher than those in yearly models. This can be attributed to the fact that there is always a lag in the change in moisture from the change in pressure head. Hence, the moisture level seen is actually an average of the moisture level from its adjoining pressure heads. In an yearly model, this average is over 365 days and hence the moisture is significantly lower than over one day.
3. Fig **5.1, 5.5, 5.9, 5.11, 5.15, 5.19, 5.23, 5.27, 5.31, 5.35, 5.39, 5.43, 5.47, 5.50 and 5.53** show the variation of groundwater levels over the time period by the change of pressure head. As seen, there is always a small delay in the change of moisture in the top soil, with respect to the change in pressure head.
4. The study for soil moisture variation cannot be conducted in a steady state, as is evident from fig **5.56**. The transient state helps to vary the pressure head on a temporal basis, so as to plot the corresponding change in soil moisture.

# REFERENCES


[1] Darcy, H. (1856). Les Fontaines Publiques de la Ville de Dijon, Dalmont, Paris

[2] Richards, L.A., Capillary conduction of fluid through porous mediums. *Physics* 1, 318-333, 1931

[3] J. Bear, *Hydraulics of Groundwater*, McGraw-Hill, 1978

[4] M.Th. van Genuchten, "A closed-form equation for predicting the hydraulic of conductivity of unsaturated soils," *Soil Sci. Soc. Am. J.*, vol. 44, pp. 892–898, 1980

[5] Feddes, R.A., P.J. Kowalik and J. Zaradny 1978. Simulation of field water use and crop yield. PUDOC, Wageningen, Simulation Monographs.

[6] Shao, M. and Horton, R. 1998. Integral method for estimating soil hydraulics properties. Soil Sci. Soc. Am. J. 62: 585-592

[7] Paniconi C, Aldama AA, Wood EF 1991 Numerical evaluation of iterative and noniterative methods for the solution of nonlinear Richards equation

[8] Lenhard, R.J., Parker, J.C. and Mishra, S. 1989. On the correspondence between Brooks-Corey and van Genuchten models. *J. Irrig. Drain. E.* 115: 744-751

[9] Hammad, J.A., Future of ground water in African Sahara, *J Irrig Drainage Div Proc Am Soc Civ Engng*, 95 (1969), pp. 563–580

[10] Werner, P.W., 1946. Notes on flow-time effects in the great artesian aquifers of the earth, *Trans. Am. Geophys. Union*, 27(5): 687--708.

[11] Massland, M., 1959. Water table fluctuations induced by intermittent recharge, *J. Geophys. Res*., 64: 549-559

[12] Gill, M.A., 1984. Water table rise due to infiltration from canals. J. Hydrol., 70: 337-352.

[13] Mustafa, S., 1987. Water table rise in a semi-confined aquifer due to surface infiltration and canal recharge. J. Hydrol., 95: 269-276

[14] Sewa Ram, C.S.J. and Chauhan, H.S., 1987a. Drainage of sloping lands with constant replenishment. J. Irrig. Drain. Eng., ASCE., 113: 213-223

[15] Sewa Ram, C.S.J. and Chauhan, H.S., 1987b. Analytical and experimental solutions for drainage of sloping lands with time varying recharge. Water Resour. Res., 23: 1090-1095.

[16] Venetis, C., Estimating infiltration and/or the parameters of unconfined aquifers from groundwater level observations. J. Hydro, 1971, 12, 161-9

[17] Onyejekwe. O.O., Unsteady free flow to an observation well from a semi-confined leaky aquifer, *Adv Engng Software*, 19 (1994), pp. 173–175

[18] Mustafa, S., 1987. Water table rise in a semi-confined aquifer due to surface infiltration and canal recharge. J. Hydrol., 95: 269-276

[19] Latinopoulos, P., The response of ground water to artificial recharge schemes, *Water Resour Res*, 17 (1981), pp. 1712–1714